IHES/P/99/90
GRP/99/521
gr-qc/0001013

Transition from inspiral to plunge in binary black hole coalescences

Alessandra Buonanno[a,b] and Thibault Damour[b,c]

[a] *Physics, Mathematics and Astronomy Department, California Institute of Technology, Pasadena, CA 91125*

[b] *Institut des Hautes Etudes Scientifiques, 91440 Bures-sur-Yvette, France*

[c] *DARC, CNRS-Observatoire de Paris, 92195 Meudon, France*

Abstract

Combining recent techniques giving non-perturbative re-summed estimates of the damping and conservative parts of the two-body dynamics, we describe the transition between the adiabatic phase and the plunge, in coalescing binary black holes with comparable masses moving on quasi-circular orbits. We give initial dynamical data for numerical relativity investigations, with a fraction of an orbit left, and provide, for data analysis purposes, an estimate of the gravitational wave-form emitted throughout the inspiral, plunge and coalescence phases.

I. INTRODUCTION

The most promising candidate sources for ground based interferometric gravitational-wave (GW) detectors such as LIGO and VIRGO are binary systems made of massive (stellar) black holes [1–4]. Such binary black holes (with individual masses in the range, say, $3-15M_\odot$) pose special problems [3], [5].

Let us recall that gravitational radiation damping is efficient at circularizing such binary systems, and then drives, for a long time, a slow inspiraling quasi-circular motion of the binary system. This quasi-circular "adiabatic inspiral phase" is expected to terminate abruptly, and to change to some type of "plunge phase" (leading to final coalescence) when the binary orbit shrinks down to the Last Stable (circular) Orbit (LSO) defined by the conservative part of the nonlinear relativistic force law between two bodies. [In the test-mass limit, the full nonlinear relativistic force law corresponds to geodesic motion in a Schwarzschild spacetime, and exhibits, as is well known, an LSO located at $R = 6GM$. One expects that a comparable-mass system will still exhibit such an LSO; see below.] Now, the signal to noise ratio (in an initial LIGO detector) for inspiral signals from comparable-mass black hole binaries reaches a *maximum* for $M \simeq 28M_\odot$, which corresponds to a GW frequency for the waves emitted at the Last Stable (circular) Orbit (LSO) equal to $f_{\rm GW}^{\rm LSO} \simeq 170$Hz, a value which is (not accidentally) very close to the location $f_{\rm det} \simeq 167$Hz (for initial LIGO) of the minimum of the characteristic detector noise amplitude $h_n(f) \equiv \sqrt{f\, S_n(f)}$ (see Fig. 1 of [5]). Therefore the first detections will probably concern massive systems with $M \sim 30M_\odot$. Moreover, Ref. [5] has shown that when the total mass $M \equiv m_1 + m_2$ lies in the range $5 - 40M_\odot$ the proximity (within a factor ~ 2) between the observationally most important frequencies[1] $f_{\rm det}$ and the GW frequency at the LSO, $f_{\rm GW}^{\rm LSO}$, was calling both for an especially careful treatment of the Fourier transform of the emitted waveform, and for an improved knowledge of the transition between the inspiral phase and the plunge phase.

The present paper will attempt to improve our knowledge of the transition between inspiral and plunge by combining two, recently proposed, *non-perturbative* techniques: Refs. [6]

[1] We neglect here the very small difference between the optimal frequency $f_{\rm det}$ for generic broad-band bursts, and the optimal frequency f_p for inspiral signals (see [5]).

and [7]. Let us first recall that, a few years ago, Will and collaborators [8], [9] tried to attack the problem of the late-time evolution of compact binaries (including the transition from inspiral to plunge) by a direct use of the Damour-Deruelle [10–12] equations of motion. These equations of motion are given in the form of a *perturbative* expansion in powers of a small parameter $\varepsilon = v/c$ ("post-Newtonian", or, in short, PN, expansion). In Ref. [8] a direct integration of these perturbative equations of motion (using the method of osculating elements) was used, while, in Ref. [9] it was proposed to improve the straightforward perturbative approach by using "hybrid" equations of motion. The "hybrid" approach is a *partial* re-summation approach in which the perturbative terms in the equations of motion which survive in the test mass limit ($\nu \equiv m_1\, m_2/(m_1+m_2)^2 \to 0$) are replaced by the known, exact "Schwarzschild terms", while the ν-dependent terms are left as a perturbative expansion. Both the robustness [13], [14] and the consistency [6] of the hybrid approach of [9] have been questioned. [In particular, it was pointed out in Ref. [6] that, in this approach, the supposedly small "ν-corrections" represent, in several cases, a very large (larger than 100%) modification of the corresponding ν-independent terms.] Another sign of the unreliability of the hybrid approach is the fact that the recent study [15,16] of the location of the LSO at the third post-Newtonian (3PN) accuracy has qualitatively confirmed the 2PN-level results of the non-perturbative techniques to be discussed below (namely that the LSO is "lower than 6GM"), thereby casting doubt on the most striking prediction of the hybrid approach (an LSO "higher than 6GM", i.e. with a lower orbital frequency).

By contrast with the perturbative approach of [8] and the partially re-summed approach of [9], the present paper will rely on the systematic use of non-perturbative re-summation techniques. The basic philosophy underlying our approach is the following. We are interested in understanding, in quantitative detail, the combined influence on the inspiral $\to$ plunge transition of radiation reaction and of non-linear effects in the force law for *comparable-mass* binary systems (i.e. for systems for which $\nu \equiv m_1\, m_2/(m_1+m_2)^2$ is around[2] 1/4).

At present there exists no method for deriving, from first principles, non-perturbative

[2] Note that because ν, considered as a function of the ratio m_1/m_2, reaches its *maximum* $\nu_{\max} = 1/4$ for $m_1/m_2 = 1$ it stays numerically near 1/4 even for mass ratios quite different from 1. E.g., even for $m_1/m_2 = 3$, $4\nu = 0.75$.

expressions for the two-body equations of motion, especially in the case of interest where 4ν is *not* a small parameter. As a substitute we shall combine two different re-summation techniques that have been recently introduced to deal with two separate aspects of the problem we wish to tackle.

The first re-summation technique, introduced in [6], allows one to get a non-perturbative, ν-dependent, estimate of the rate of loss of angular momentum (under gravitational damping) in quasi-circular, comparable-mass binaries. The idea of [6] is three-pronged: (i) to work with an invariant function of an invariant argument, $F(v)$, (ii) to inject some plausible information about the meromorphic structure of this function, and, finally, (iii) to use Padé approximants to estimate $F(v)$ from the first few known terms in the perturbative (PN) expansion of $F(v)$. The second re-summation technique, introduced in [7], allows one to derive a non-perturbative, ν-dependent, estimate of the (conservative part of the) nonlinear force law determining the motion of comparable binaries. The idea of [7] is to map the real two-body problem on a simpler effective one-body problem, i.e. on the problem of the motion of a particle of mass $\mu \equiv m_1 m_2/(m_1+m_2)$ in some "effective" background metric $g^{\rm eff}_{\mu\nu}(x^\lambda)$. The possibility (and uniqueness, given some natural requirement) of such a mapping, real $\to$ effective, was proven at the 2PN level in [7]. The extension of this approach at the 3PN level has been recently discussed [15,16] on the basis of the 3PN dynamics recently derived by Jaranowski and Schäfer [17]. At the 2PN level the ν-dependent terms in the effective metric were found to be numerically so small (around the LSO) that the need for a further (Padé-type) re-summing of the effective metric coefficients did not arise. [However, note that Ref. [16] has introduced, at 2PN and 3PN, the further idea of a specific, Padé-improvement of $g^{\rm eff}_{\mu\nu}(x^\lambda)$.] In this paper we shall show how one can combine the methods of [6] and [7] to derive a full force law (including radiation reaction) describing the quasi-circular motion of comparable-mass binaries. Our approach is intended to apply to any value of ν, but is restricted to considering *quasi-circular* motions, where the radial velocity $\dot{R}$ is much smaller than the circular one $R\,\dot{\varphi}$. As we shall see, we shall consistently check that the condition $\dot{R} \ll R\,\dot{\varphi}$ holds true not only during the adiabatic inspiral, but also during the transition to the plunge, and even during most of the plunge.

We apply our method, in this paper, to deriving two sorts of results which are of direct interest to the ongoing effort to detect gravitational waves. First, we shall give initial dynamical data (i.e. initial positions and momenta) for binary black holes that have just

started their plunge motion. The idea here is that numerical relativity will probably not be able, before quite a few years, to accurately evolve binary systems over many (or even ~ 10) orbits. This is why we propose a method for computing accurate initial dynamical data at a moment so late in the evolution that there remains (when $4\nu \sim 1$) *less* than one orbit to evolve. [In the equal-mass case, $\nu = 1/4$, we shall compute data $\simeq 0.6$ orbit before "coalescence".] Our contention (whose robustness we shall try to establish) is that suitably re-summed versions of *analytic* (PN) results allow one to push the evolution that far. [We shall use here 2.5PN-accurate information for angular momentum loss and 2PN-accurate information for the conservative force law. However, as shown in [6] and [15,16] our method can be pushed to higher accuracy when the correspondingly needed PN results become unambiguously known.] Note that this attitude is opposite to the one taken in [3] in which it was assumed that "there is little hope, via PN Padé approximants, to evolve" a binary system up to the moment where it can provide initial data for the final coalescence. Let us, however, immediately add that the present paper is still incomplete, in that we give only dynamical data $(\boldsymbol{q}_1, \boldsymbol{q}_2, \boldsymbol{p}_1, \boldsymbol{p}_2)$ but we do not solve the remaining problem of constructing the initial gravitational data $(g_{ij}(x), K_{ij}(x))$ determined (in principle) by $(\boldsymbol{q}_a, \boldsymbol{p}_a)$ (given, say, some no-incoming-radiation condition). We shall leave this (important) issue to future work.

The second aim of this work is to provide, for data analysis purposes, some estimate of the complete waveform emitted by the coalescence of two black holes (with negligible spins). We do not claim that this part of the work will be as accurate as the first one. The idea here is to provide a (hopefully $\sim 10\%$ accurate) guess of the complete waveform, with its transition from an inspiral phase to a plunge one, followed by a coalescence ending in a stationary final state. In view of the recent realization [5] of the crucial importance of the details of the transition to the plunge for the construction of faithful GW templates (for massive binaries with $5M_\odot \lesssim M \lesssim 40M_\odot$) even an approximate knowledge of the complete waveform will be a valuable information for data analysis (e.g. to test the accuracy of present templates, and/or to propose more accurate or, at least, more robust, templates).

While preparing this work for publication, we learned of the existence of an independent work of Ori and Thorne [18] which deals with the transition between the inspiral and the plunge in the test mass limit ($\nu \to 0$).

II. CONSERVATIVE PART OF THE TWO-BODY FORCE LAW

In this section, we recall the non-perturbative construction of the (conservative) two-body force law given in Ref. [7]. There it was shown that the conservative part (i.e. without radiation damping) of the dynamics of a binary system, represented in ADM phase-space coordinates $(\boldsymbol{q}_1^{\rm ADM}, \boldsymbol{q}_2^{\rm ADM}, \boldsymbol{p}_1^{\rm ADM}, \boldsymbol{p}_2^{\rm ADM})$, could be mapped (at the 2PN level), via the combination of an energy map, $\mathcal{E}_{\rm eff} = f\,(\mathcal{E}_{\rm real})$, and a canonical transformation, $(\boldsymbol{q}_a^{\rm ADM}, \boldsymbol{p}_a^{\rm ADM}) \to (\boldsymbol{q}_a, \boldsymbol{p}_a)$, $a = 1, 2$, into the simpler dynamics of the geodesic motion of a particle of mass $\mu = m_1\, m_2/(m_1 + m_2)$ in some effective background geometry $g^{\rm eff}_{\mu\nu}(x)$:

$$ds^2_{\rm eff} = g^{\rm eff}_{\mu\nu}(x^\lambda)\, dx^\mu\, dx^\nu = -A(R)\, c^2\, dt^2 + B(R)\, dR^2 + C(R)\, R^2\, (d\theta^2 + \sin^2\theta\, d\varphi^2)\,. \qquad (2.1)$$

[See [16] for the generalization of this approach to the 3PN level.] Here the coordinates (R, θ, φ) are polar coordinates in the *effective* problem (describing the relative motion). They are related in the standard way ($Q^x = R\,\sin\theta\,\cos\varphi$, $Q^y = R\,\sin\theta\,\sin\varphi$, $Q^z = R\,\cos\theta$) to the (relative) effective Cartesian coordinates $\boldsymbol{Q} = \boldsymbol{q}_1 - \boldsymbol{q}_2$, where $\boldsymbol{q}_1$ and $\boldsymbol{q}_2$ are the effective coordinates of each body. One works in the center-of-mass frame of the binary system, i.e. $\boldsymbol{p}_1 + \boldsymbol{p}_2 = 0 = \boldsymbol{p}_1^{\rm ADM} + \boldsymbol{p}_2^{\rm ADM}$. The canonical conjugate of the relative position $\boldsymbol{Q}$ is the relative momentum $\boldsymbol{P} = \boldsymbol{p}_1 = -\boldsymbol{p}_2$. In most of this paper we shall work with the effective phase-space coordinates $(\boldsymbol{Q}, \boldsymbol{P})$ [or rather with scaled versions of their polar [3] counterparts $(R, \theta, \varphi; P_R, P_\theta, P_\varphi)$]. We shall only discuss at the end how to construct the more physically relevant ADM phase space coordinates $(\boldsymbol{q}_a^{\rm ADM}, \boldsymbol{p}_a^{\rm ADM})$ from $(\boldsymbol{Q}, \boldsymbol{P})$.

In absence of damping (to be added later), the evolution (with respect to the real ADM time coordinate $t_{\rm real}$) of $(\boldsymbol{Q}, \boldsymbol{P})$ is given by Hamilton's equations

$$\frac{dQ^i}{dt_{\rm real}} - \frac{\partial H^{\rm improved}_{\rm real}(\boldsymbol{Q}, \boldsymbol{P})}{\partial P_i} = 0\,, \qquad (2.2)$$

$$\frac{dP_i}{dt_{\rm real}} + \frac{\partial H^{\rm improved}_{\rm real}(\boldsymbol{Q}, \boldsymbol{P})}{\partial Q^i} = 0\,, \qquad (2.3)$$

where the *real* (i.e. giving the $t_{\rm real}$-evolution, and the real two-body energy) *improved* (i.e. representing a non-perturbative re-summed estimate of the real PN Hamiltonian) Hamiltonian reads

---

[3] Note that we have the usual relations, such as, $P_R = n^i\, P_i$ with $n^i = Q^i/R$, and $P_\varphi = Q^x\, P_y - Q^y\, P_x$.

$$H^{\rm improved}_{\rm real}(\boldsymbol{Q},\boldsymbol{P}) = M\,c^2\,\sqrt{1+2\nu\,\left(\frac{H_{\rm eff}(\boldsymbol{Q},\boldsymbol{P})-\mu\,c^2}{\mu\,c^2}\right)}\,, \tag{2.4}$$

and

$$H_{\rm eff}(\boldsymbol{Q},\boldsymbol{P}) = \mu\,c^2\,\sqrt{A(Q)\,\left[1+\frac{(\boldsymbol{n}\cdot\boldsymbol{P})^2}{\mu^2\,c^2\,B(Q)}+\frac{(\boldsymbol{n}\times\boldsymbol{P})^2}{\mu^2\,c^2\,C(Q)}\right]}\,. \tag{2.5}$$

Here $Q \equiv \sqrt{\delta_{ij}\,Q^i\,Q^j} = R$, $n^i = Q^i/Q$ is the unit vector in the radial direction, and the scalar and vector products are performed as in Euclidean space. Henceforth, we shall pose $t \equiv t_{\rm real}$, $H \equiv H^{\rm improved}_{\rm real}$ and use the following notation:

$$M \equiv m_1 + m_2\,, \qquad \mu \equiv \frac{m_1\,m_2}{M}\,, \qquad \nu \equiv \frac{\mu}{M} \equiv \frac{m_1\,m_2}{(m_1+m_2)^2}\,. \tag{2.6}$$

In polar coordinates, restricting ourselves to planar motion in the equatorial plane $\theta = \pi/2$ and to the Schwarzschild gauge ($C(Q)=1$), we get the equations of motion

$$\frac{dR}{dt} = \frac{\partial H}{\partial P_R}(R,P_R,P_\varphi)\,, \tag{2.7}$$

$$\frac{d\varphi}{dt} = \frac{\partial H}{\partial P_\varphi}(R,P_R,P_\varphi)\,, \tag{2.8}$$

$$\frac{dP_R}{dt} + \frac{\partial H}{\partial R}(R,P_R,P_\varphi) = 0\,, \tag{2.9}$$

$$\frac{dP_\varphi}{dt} = 0\,, \tag{2.10}$$

with

$$H(R,P_R,P_\varphi) = M\,c^2\,\sqrt{1+2\nu\,\left[\sqrt{A(R)\,\left(1+\frac{P_R^2}{\mu^2\,c^2\,B(R)}+\frac{P_\varphi^2}{\mu^2\,c^2\,R^2}\right)}-1\right]}\,. \tag{2.11}$$

Like in any (non-degenerate) Hamiltonian system, this conservative dynamics is equivalent to a Lagrangian dynamics

$$L^{\rm improved}_{\rm real}(\boldsymbol{Q},\dot{\boldsymbol{Q}}) = P_i\,\dot{Q}^i - H^{\rm improved}_{\rm real}(\boldsymbol{Q},\boldsymbol{P})\,, \tag{2.12}$$

with $P_i(\dot{Q})$ obtained by solving $\dot{Q}^i = \partial H/\partial P_i$. The Lagrangian equations of motion read:

$$\frac{d}{dt}\,\frac{\partial L^{\rm improved}_{\rm real}}{\partial \dot{Q}^i} - \frac{\partial L^{\rm improved}_{\rm real}}{\partial Q^i} = 0\,. \tag{2.13}$$

To ease the notation we denote $L \equiv L^{\rm improved}_{\rm real}$.

Finally, the 2PN-accurate metric coefficients $A(R)$, $B(R)$, Eq. (2.1), (in the Schwarzschild gauge where $C(R) \equiv 1$) read

$$A(R) = 1 - \frac{2\,GM}{c^2\,R} + 2\nu \left(\frac{GM}{c^2\,R}\right)^3 , \tag{2.14}$$

$$B(R) \equiv D(R)/A(R)\,, \tag{2.15}$$

with

$$D(R) = 1 - 6\nu \left(\frac{GM}{c^2\,R}\right)^2 . \tag{2.16}$$

Note that it was recently suggested [16] (because of the slow convergence of the 3PN contributions) to replace the straightforward expression (2.14) by a suitably Padeed version, namely (at 2PN): $A_{P_2}(R) = 1 - 2u(1 + \nu u^2)^{-1}$, where $u \equiv GM/c^2\,R$. However, we have checked that this refinement has only a very minor effect on the results to be discussed below.

The re-summed (conservative) dynamics defined by the Hamiltonian (2.11) contains a Last Stable (circular) Orbit (LSO) which is a ν-deformed version of the well known Schwarzschild LSO. Let us recall that the radius of the LSO is obtained by imposing the existence of an inflection point in the effective potential $H(R, P_R = 0, \mathcal{J})$ for the radial motion,

$$\frac{\partial H}{\partial R}\,(R, P_R = 0, \mathcal{J}) = 0 = \frac{\partial^2 H}{\partial R^2}\,(R, P_R = 0, \mathcal{J})\,, \tag{2.17}$$

where the total angular momentum $\mathcal{J} \equiv P_\varphi$ stays fixed. Eq. (2.17) has a solution in R (for each value of ν) only for some specific value of $\mathcal{J} = \mathcal{J}^{\rm LSO}(\nu)$. In terms of the rescaled variables $r \equiv c^2 R/GM$, $j \equiv c\mathcal{J}/(\mu\,GM)$, $\widehat{\omega} \equiv GM\,\dot{\varphi}/c^3$, the LSO quantities defined, in the equal-mass case $\nu = 1/4$, by the Hamiltonian (2.11), take the following values [7]

$$\begin{aligned} & r_{\rm LSO}\,(1/4) = 5.718\,, \qquad && j_{\rm LSO}\,(1/4) = 3.404\,, \\ & \widehat{\omega}_{\rm LSO}\,(1/4) = 0.07340\,, \qquad && \frac{\mathcal{E}^{\rm LSO}_{\rm real}\,(1/4) - Mc^2}{Mc^2} = -0.01501\,. \end{aligned} \tag{2.18}$$

Note that the comparable-mass LSO is slightly more inwards (both in terms of the coordinate R and in the sense of having a higher orbital frequency) than its corresponding rescaled test-mass limit: $r_{\rm LSO}(0) = 6$, $j_{\rm LSO}(0) = \sqrt{12} = 3.4641$, $\widehat{\omega}_{\rm LSO}(0) = 6^{-3/2} = 0.068041$.

As we shall need in the following to refer to the numerical value of $\widehat{\omega}_{\rm LSO}(\nu)$ for arbitrary values of ν, we have fitted the result obtained by the (rather intricate) method of Ref. [7] to a simple polynomial in ν. We find

$$\widehat{\omega}_{\rm LSO}(\nu) \simeq \omega_0 \left[1 + \omega_1 \left(4\nu\right) + \omega_2 \left(4\nu\right)^2\right], \tag{2.19}$$

$$\omega_0 = 0.0680414\,, \qquad \omega_1 = 0.0693305\,, \qquad \omega_2 = 0.00935142\,. \tag{2.20}$$

III. INCORPORATING RADIATION REACTION EFFECTS

We wish to augment the conservative dynamics described in the previous section by adding, as accurately as possible, radiation reaction effects. If we were doing it in the Lagrangian formalism we would write (in any coordinate system)

$$\frac{d}{dt}\frac{\partial L}{\partial \dot{Q}^i} - \frac{\partial L}{\partial Q^i} = \mathcal{F}_i^{\rm Lag}(Q, \dot{Q})\,. \tag{3.1}$$

This would define the additional damping force $\mathcal{F}_i^{\rm Lag}(Q, \dot{Q})$ needed in the Lagrangian formalism. In particular, in polar coordinates we would write (for planar motion $\theta = \pi/2$):

$$\frac{d}{dt}\frac{\partial L}{\partial \dot{R}} - \frac{\partial L}{\partial R} = \mathcal{F}_R^{\rm Lag}(R, \varphi, \dot{R}, \dot{\varphi})\,, \tag{3.2}$$

$$\frac{d}{dt}\frac{\partial L}{\partial \dot{\varphi}} = \mathcal{F}_\varphi^{\rm Lag}(R, \varphi, \dot{R}, \dot{\varphi})\,. \tag{3.3}$$

We want to work in the Hamiltonian framework, hence coming back to the coordinates R, P_R, φ and P_φ and imposing the constraint that the usual definition $P_i = \partial L/\partial \dot{Q}^i$ holds without corrections (which implies that the other usual relations $\dot{Q}^i = \partial H/\partial P_i$, $\partial H/\partial Q^i = -\partial L/\partial Q^i$ and Eq. (2.12) hold too) we get

$$\frac{dR}{dt} - \frac{\partial H}{\partial P_R}(R, P_R, P_\varphi) = 0\,, \tag{3.4}$$

$$\frac{d\varphi}{dt} - \frac{\partial H}{\partial P_\varphi}(R, P_R, P_\varphi) = 0\,, \tag{3.5}$$

$$\frac{dP_R}{dt} + \frac{\partial H}{\partial R}(R, P_R, P_\varphi) = \mathcal{F}_R^{\rm Ham}(R, \varphi, P_R, P_\varphi)\,, \tag{3.6}$$

$$\frac{dP_\varphi}{dt} = \mathcal{F}_\varphi^{\rm Ham}(R, \varphi, P_R, P_\varphi)\,, \tag{3.7}$$

where the Hamiltonian damping force $\mathcal{F}_i^{\rm Ham}(Q^j, P_j)$ is numerically equal to the Lagrangian one: $\mathcal{F}_i^{\rm Ham}(Q^j, P_j) = \mathcal{F}_i^{\rm Lag}(Q^j, \dot{Q}^j = \partial H/\partial P_j)$.

A. What do we know about the radiation reaction force?

The radiation reaction force $\mathcal{F}$ was computed explicitly, at lowest (Newtonian) fractional order, in harmonic Cartesian-like coordinates, as part of the complete 2.5PN equations of motion, by Damour and Deruelle [10–12]. An equivalent result was also derived within the ADM canonical formalism by Schäfer [19–21]. At higher post-Newtonian orders one has only an incomplete knowledge of the equations of motion, and one has to rely on the (assumed) balance between energy and angular momentum losses in the system and at infinity [22,23]. To get an idea of the generic structure of the radiation damping (in various coordinate systems, and at various PN approximations) let us consider the general radiation reaction force written (at 1PN fractional accuracy; and setting $G = 1$) by Iyer and Will [22].

$$\mathcal{F}_i^{\rm Lag} = \mu \left[\alpha(R,v)\, \dot{R}\, n^i + \beta(R,v)\, v^i \right] , \tag{3.8}$$

$$\alpha(R,v) = \frac{8}{5}\,\nu\,\frac{M}{R^2}\,\frac{M}{R}\,(A_{5/2} + A'_{7/2} + \cdots) , \tag{3.9}$$

$$\beta(R,v) = -\frac{8}{5}\,\nu\,\frac{M}{R^2}\,\frac{M}{R}\,(B_{5/2} + B'_{7/2} + \cdots) , \tag{3.10}$$

where R is the relative radius and v is the velocity. Then, using post-Newtonian expressions for the energy and the angular momentum flux at infinity, and assuming energy and angular momentum balance, they obtained at lowest (Newtonian) fractional order

$$A_{5/2} = 3\,(1+\overline{\beta})\,v^2 + \frac{1}{3}\,(23 + 6\,\overline{\alpha} - 9\,\overline{\beta})\,\frac{M}{R} - 5\,\overline{\beta}\,\dot{R}^2 , \tag{3.11}$$

$$B_{5/2} = (2+\overline{\alpha})\,v^2 + (2-\overline{\alpha})\,\frac{M}{R} - 3\,(1+\overline{\alpha})\,\dot{R}^2 . \tag{3.12}$$

See Ref. [22] for the expressions of the 1PN-accurate radiation damping terms $A_{7/2}$ and $B_{7/2}$ in the equations of motion (equivalent, after some reshuffling, with the Lagrangian contributions $A'_{7/2}$, $B'_{7/2}$ in Eqs. (3.9), (3.10)).

The coefficients $\overline{\alpha}$ and $\overline{\beta}$ that appear in Eqs. (3.11) and (3.12) are two arbitrary gauge parameters that cannot be fixed by the energy balance method. Iyer and Will [22] showed that this gauge freedom is equivalent to shifting the (conservative) coordinate system by small radiative corrections. Let us notice that the gauge dependence is reduced when considering quasi-circular orbits. Indeed, in that case $\dot{R}^2 \simeq 0$, $M/R \simeq v^2$ and Eqs. (3.9), (3.10) become (considering only the 5/2PN terms which are sufficient for the point we wish to make)

$$\alpha_{\rm circ} \simeq \frac{8}{5}\,\nu\,\frac{M}{R^2}\,\left(\frac{M}{R}\right)^2\,\left(\frac{32}{3} + 2\,\overline{\alpha}\right) , \qquad \beta_{\rm circ} \simeq -\frac{32}{5}\,\nu\,\frac{M}{R^2}\,\left(\frac{M}{R}\right)^2 . \tag{3.13}$$

Hence, in the quasi-circular case the only gauge-dependence left is in the coefficient $\alpha(R,v)$ multiplying the *radial* component of the damping force ($\propto n^i$). We can use this gauge arbitrariness to set the ratio

$$\left(\frac{\alpha}{\beta}\right)_{\rm circ.} \simeq -\frac{1}{2}\left(\frac{16}{3}+\overline{\alpha}\right), \tag{3.14}$$

to any value we like. For example, by choosing $\overline{\alpha}=-16/3$ we can set $\alpha_{\rm circ.}=0$ or by choosing $\overline{\alpha}=-10/3$ we can set $(\alpha+\beta)_{\rm circ.}=0$.

Having understood the gauge dependence of the coefficient α in Eq. (3.8) let us come back to the general structure (3.8) (considered at any PN accuracy, with some (unknown) coefficients α and β). The polar-coordinate version (for planar motion $\theta=\pi/2$) of the Cartesian-like Lagrangian damping force (3.8) reads (3.2), (3.3) with

$$\mathcal{F}_R^{\rm Lag}=\mathcal{F}_i^{\rm Lag}\frac{\partial Q^i}{\partial R}=n^i\,\mathcal{F}_i^{\rm Lag}\,, \tag{3.15}$$

$$\mathcal{F}_\varphi^{\rm Lag}=\mathcal{F}_i^{\rm Lag}\frac{\partial Q^i}{\partial \varphi}=Q^x\,\mathcal{F}_y^{\rm Lag}-Q^y\,\mathcal{F}_x^{\rm Lag}. \tag{3.16}$$

This yields

$$\mathcal{F}_\varphi^{\rm Lag}=\mu\,\beta\,R^2\,\dot\varphi\,,\qquad \mathcal{F}_R^{\rm Lag}=\mu\,(\alpha+\beta)\,\dot R\,. \tag{3.17}$$

The important information for our present purpose is the difference between the φ-component of the damping force, which contains only β and is, therefore, gauge-independent [4], and the R-component which contains the gauge-dependent combination $\alpha+\beta$. Let us note, in particular, the expression of the ratio

$$\frac{\mathcal{F}_R^{\rm Lag}}{\mathcal{F}_\varphi^{\rm Lag}}=\left(\frac{\alpha}{\beta}+1\right)\frac{\dot R}{R^2\,\dot\varphi}\,. \tag{3.18}$$

In the following we shall be interested in quasi-circular motions with $\dot R\ll R\,\dot\varphi$. [We shall see that this condition remains satisfied even during part of the plunge phase.] As we see from Eq. (3.18), for such motions the radial component of the damping force will contain

[4]The discussion above concerns only the lowest-order term in β, but we shall see below that, to all orders, the crucial combination $\beta\,R^2$ can, for circular orbits, be expressed in terms of invariant quantities.

one power of the small dimensionless quantity $\dot{R}/(R\,\dot{\varphi})$. But we learned above, from the gauge dependence of the lowest-order damping force, that we can change the definition of the radial coordinate so as to set, for instance, the quantity $(\alpha/\beta)+1$ to zero (for circular orbits). This means that the RHS of Eq. (3.18) can be arranged, in the case of quasi-circular orbits, to contain three powers of the small parameter $\dot{R}/(R\,\dot{\varphi})$. (From Eqs. (3.11), (3.12) we see that for quasi-circular orbits $\alpha+\beta \propto \dot{R}^2$.) We have checked that the reasoning made above, using the lowest-order gauge dependence, can be formally extended to all higher PN orders.

The conclusion is that there should exist a special coordinate gauge where, for quasi-circular motions, an excellent approximation to the damping force is obtained by replacing the radial component simply by zero:

$$\mathcal{F}_R^{\rm Lag} = 0 = \mathcal{F}_R^{\rm Ham}\,. \tag{3.19}$$

To test, a posteriori, the robustness of the approximation (3.19), we shall also consider another special gauge: namely that where $(\alpha/\beta)_{\rm circ}=0$. [As we said above, this can be achieved at lowest order by a suitable choice of $\overline{\alpha}$, and this can be extended to higher PN orders by suitable choices of higher gauge parameters.] Finally, this means that there exists another coordinate gauge where, to an excellent approximation, the radial damping force is given as

$$\mathcal{F}_R^{\rm Lag} = \mathcal{F}_R^{\rm Ham} = \frac{\dot{R}}{R^2\,\dot{\varphi}}\,\mathcal{F}_\varphi^{\rm Ham}\,. \tag{3.20}$$

The results in the two gauges are compared and discussed at the end of Sec. V.

What is important for the following is that in both gauges (3.19) or (3.20), the knowledge of the full damping force can be deduced from the sole knowledge of $\mathcal{F}_\varphi$.

B. Non-perturbative estimate of the angular momentum reaction force along quasi-circular orbits

The analysis of the previous subsection has shown that the crucial equation in which one should accurately incorporate radiation reaction effects is

$$\frac{dP_\varphi}{dt} = \mathcal{F}_\varphi^{\rm Ham}(R,\varphi,P_R,P_\varphi)\,. \tag{3.21}$$

As P_φ is just the total angular momentum of the binary system, Eq. (3.21) expresses the rate of loss of angular momentum under gravitational radiation reaction. As usual we shall estimate the RHS $\mathcal{F}_\varphi = \mathcal{F}_\varphi^{\rm Ham} = \mathcal{F}_\varphi^{\rm Lag}$ (remember that $\mathcal{F}^{\rm Ham}$ and $\mathcal{F}^{\rm Lag}$ differ only in the arguments in which they are expressed) by assuming that there is a balance between the mechanical angular momentum lost by the system, and the flux of angular momentum at infinity in the form of gravitational waves. In the case of interest here of quasi-circular orbits we expect that, to a good approximation, $\mathcal{F}_\varphi$ will not depend explicitly on φ and will, therefore, be expressible in terms of the *orbit-averaged* flux of angular momentum. Moreover, in the case of quasi-circular orbits there is a simple relation between angular-momentum-loss and energy-loss. Indeed, the rate of energy-loss along any orbit, in polar coordinates, is given by

$$\frac{d\mathcal{E}}{dt} = \frac{dH}{dt} = \dot{R}\,\mathcal{F}_R + \dot{\varphi}\,\mathcal{F}_\varphi\,, \tag{3.22}$$

and in particular along quasi-circular orbit we have (remembering Eq. (3.18))

$$\left(\frac{dH}{dt}\right)_{\rm quasi-circ.} \simeq \dot{\varphi}\,\mathcal{F}_\varphi^{\rm circ.} + \mathcal{O}(\dot{R}^2)\,. \tag{3.23}$$

Finally, if we know some good estimate of the (averaged) energy-loss along circular orbits, say

$$\left(\frac{dH}{dt}\right)_{\rm circ.} \simeq -\Phi_{\rm circ.}(\dot{\varphi})\,, \tag{3.24}$$

we can obtain a good estimate of the needed φ-reactive force

$$\mathcal{F}_\varphi^{\rm circ.} \simeq -\frac{\Phi_{\rm circ.}(\dot{\varphi})}{\dot{\varphi}}\,. \tag{3.25}$$

The problem of giving a non-perturbative, re-summed estimate of the energy-loss-rate (or "flux function") along circular orbits, say $\Phi_{\rm circ}$, has been recently tackled by Damour, Iyer and Sathyaprakash [6]. By combining several of the non-perturbative techniques recalled above (to work with an invariant function $F(v)$, to use some global information about $F(v)$ in the complex v-plane, to use Padé approximants) Ref. [6] came up with the following expression for $\Phi_{\rm circ}$, considered as a function of the gauge-invariant observable

$$v_\omega \equiv (GM\,\omega/c^3)^{1/3}\,; \qquad \omega \equiv \dot{\varphi}\,, \tag{3.26}$$

namely,

$$\Phi_{\rm circ.} = F_{\rm DIS}(v_\omega) = \frac{32}{5G}\,\nu^2\,v_\omega^{10}\,\frac{\widehat{f}_{\rm DIS}(v_\omega;\nu)}{1-v_\omega/v_{\rm pole}(\nu)}\,. \tag{3.27}$$

Here, and in the following, we set $c=1$ to simplify formulas. The function $\widehat{f}_{\rm DIS}(v_\omega;\nu)$ entering Eq. (3.27) is the "factored flux function" of [6], scaled to the Newtonian (quadrupole) flux (hence the caret on $f_{\rm DIS}$). It was shown in [6] that the sequence of near-diagonal Padé approximants of $\widehat{f}_{\rm DIS}(v)$ exhibits a very good convergence (at least in the $\nu=0$ limit where high-order PN expansions are known [24]) toward the exact result (numerically known when $\nu=0$ [25]). On this basis, it was argued in [6] that, in the comparable-mass case, $\nu\neq 0$, our "best estimate" of $\widehat{f}$ is obtained by Padeeing the currently most complete post-Newtonian results, namely the 2.5PN ones [26]. This yields a result of the form

$$\widehat{f}_{\rm DIS}(v;\nu) = \frac{1}{1+\frac{c_1\,v}{1+\frac{c_2\,v}{1+\frac{c_3\,v}{1+\frac{c_4\,v}{1+c_5\,v}}}}}\,, \tag{3.28}$$

where the dimensionless coefficients c_i depend only on ν. The c_k's are some explicit functions of the coefficients f_k of the straightforward Taylor expansion of $\widehat{f}(v)$. In turn, the f_k's, being defined by the identity (where T means "Taylor expansion")

$$T\,[\widehat{f}(v)] \equiv T\left[\left(1-\frac{v}{v_{\rm pole}}\right)\,\widehat{F}(v)\right] = 1+f_1 v+f_2 v^2+\cdots \tag{3.29}$$

are given by

$$f_k = F_k - F_{k-1}/v_{\rm pole} \tag{3.30}$$

in terms of the Taylor coefficients of the usual (Newton-normalized) flux function

$$T\,[\widehat{F}(v)] \equiv T\left[\frac{5G}{32\,\nu^2\,v^{10}}\,F(v)\right] = 1+F_2 v^2+F_3 v^3+\cdots\,. \tag{3.31}$$

[Note that $F_1=0$, but that $f_1=-1/v_{\rm pole}\neq 0$.] More explicitly we have

$$F_2 = -\frac{1247}{336}-\frac{35}{12}\,\nu\,,\qquad F_3 = 4\pi\,, \tag{3.32}$$

$$F_4 = -\frac{44711}{9072}+\frac{9271}{504}\,\nu+\frac{65}{18}\,\nu^2\,,\qquad F_5 = -\left(\frac{8191}{672}+\frac{535}{24}\,\nu\right)\,\pi\,, \tag{3.33}$$

and

$$c_1 = -f_1\,, \qquad c_2 = f_1 - \frac{f_2}{f_1}\,, \qquad c_3 = \frac{f_1\,f_3 - f_2^2}{f_1\,(f_1^2 - f_2)}\,, \tag{3.34}$$

$$c_4 = -\frac{f_1\,(f_2^3 + f_3^2 + f_1^2\,f_4 - f_2\,(2\,f_1\,f_3 + f_4))}{(f_1^2 - f_2)\,(f_1\,f_3 - f_2^2)}\,, \tag{3.35}$$

$$c_5 = -\frac{(f_1^2 - f_2)\,(-f_3^3 + 2 f_2\,f_3\,f_4 - f_1\,f_4^2 - f_2^2\,f_5 + f_1\,f_3\,f_5)}{(f_1\,f_3 - f_2^2)\,(f_2^3 + f_3^2 + f_1^2\,f_4 - f_2\,(2\,f_1\,f_3 + f_4))}\,. \tag{3.36}$$

As is clear from these expressions, they depend on the definition used for the quantity $v_{\rm pole}(\nu)$ which represents a ν-dependent estimate of the location of the "pole" in $\Phi_{\rm circ}$, which coincides (see the discussion in [6]) with the location of the "light-ring" or last unstable circular orbit ($R^{\rm Schw.}_{\rm light-ring} = 3GM$ in the $\nu \to 0$ limit). Actually, as we shall use the Padé representation only above and around the LSO ($R^{\rm Schw.}_{\rm LSO} = 6GM$ when $\nu = 0$) the precise choice of $v_{\rm pole}(\nu)$ is probably not crucial (as long as it stays near its known $\nu = 0$ limit: $v_{\rm pole}(\nu = 0) = 1/\sqrt{3}$). In this work, we shall follow Ref. [6] and use the pole location they obtained from Padeing their "new" energy function $e(x)$, namely

$$v^{\rm DIS}_{\rm pole} = \frac{1}{\sqrt{3}} \sqrt{\frac{1 + \frac{1}{3}\,\nu}{1 - \frac{35}{36}\,\nu}}\,. \tag{3.37}$$

Then, combining Eqs. (3.25), (3.26) and (3.27) we define our best estimate of the φ-component of the radiation reactive force along quasi-circular orbits as:

$$\mathcal{F}^{\rm circ.}_{\varphi} \equiv -\frac{GM}{v_\omega^3}\,\Phi_{\rm DIS}(v_\omega) = -\frac{32}{5}\,\mu\,\nu\,v_\omega^7\,\frac{\widehat{f}_{\rm DIS}(v_\omega;\nu)}{1 - v_\omega/v^{\rm DIS}_{\rm pole}(\nu)}\,. \tag{3.38}$$

To ease the notation we shall work in the following with reduced quantities, that is:

$$r \equiv \frac{R}{G\,M}\,, \qquad p_r \equiv \frac{P_R}{\mu}\,, \qquad p_\varphi \equiv \frac{P_\varphi}{\mu\,G\,M} = \frac{\mathcal{J}}{\mu\,G\,M} \equiv j\,, \tag{3.39}$$

$$\hat{t} \equiv \frac{t}{G\,M}\,, \qquad \widehat{H} \equiv \frac{H^{\rm improved}_{\rm real}}{\mu}\,, \qquad \widehat{H}_{\rm eff} \equiv \frac{H_{\rm eff}}{\mu}\,. \tag{3.40}$$

Finally, the dynamics, including radiation reaction, in re-scaled coordinates, is explicitly described by the following system of equations (in the "canonical" case where Eq. (3.19) holds)

$$\frac{dr}{d\hat{t}} = \frac{\partial \widehat{H}}{\partial p_r}(r, p_r, p_\varphi)\,, \tag{3.41}$$

$$\frac{d\varphi}{d\hat{t}} = \widehat{\omega} \equiv \frac{\partial \widehat{H}}{\partial p_\varphi}(r, p_r, p_\varphi)\,, \tag{3.42}$$

$$\frac{dp_r}{d\hat{t}} + \frac{\partial \widehat{H}}{\partial r}(r, p_r, p_\varphi) = 0\,, \tag{3.43}$$

$$\frac{dp_\varphi}{d\hat{t}} = \widehat{\mathcal{F}}_\varphi(\widehat{\omega}(r, p_r, p_\varphi))\,, \tag{3.44}$$

with

$$\widehat{H} = \frac{1}{\nu}\sqrt{1 + 2\nu\,\left[\sqrt{A(r)\,\left(1 + \frac{p_r^2}{B(r)} + \frac{p_\varphi^2}{r^2}\right)} - 1\right]}\,, \tag{3.45}$$

$$\widehat{\mathcal{F}}_\varphi(v_\omega \equiv \widehat{\omega}^{1/3}) = \frac{\mathcal{F}_\varphi}{\mu} = -\frac{32}{5}\,\nu\,v_\omega^7\,\frac{\widehat{f}_{\rm DIS}(v_\omega;\nu)}{1 - v_\omega/v_{\rm pole}^{\rm DIS}(\nu)}\,, \tag{3.46}$$

and where in Eq. (3.45) we use the scaled versions of our current best estimate of the effective metric coefficients $A(r)$, $B(r)$, see [7] and Eqs. (2.14)–(2.16) above, that is

$$A(r) \equiv 1 - \frac{2}{r} + \frac{2\nu}{r^3}\,, \qquad B(r) \equiv \frac{1}{A(r)}\,\left(1 - \frac{6\nu}{r^2}\right)\,. \tag{3.47}$$

Note that the argument v_ω entering $\widehat{\mathcal{F}}_\varphi$, Eq. (3.46), is simply defined as $v_\omega \equiv \widehat{\omega}^{1/3}$, where $\widehat{\omega} \equiv \omega\,(GM)$ is the function of r, p_r and p_φ defined by Eq. (3.42), i.e. $\widehat{\omega}(r, p_r, p_\varphi) \equiv \partial \widehat{H}(r, p_r, p_\varphi)/\partial p_\varphi$.

IV. TRANSITION BETWEEN INSPIRAL AND PLUNGE

The first-order evolution system (3.41)–(3.44) defines our proposed best estimate for completing the usually considered "adiabatic" inspiral evolution into a system which exhibits a smooth transition between inspiral and plunge. The rest of this paper will be devoted to extracting some of the important information contained in this new evolution system. Before coming to grips with such detailed information, it is useful to have a first visual impression of the physics contained in our system (3.41)–(3.44). To do this we plot on the left panel of Fig. 1 the result of a full numerical evolution of Eqs. (3.41)–(3.44) in the equal-mass case ($\nu = 1/4$). We started the evolution at $r = 15$, $\varphi = 0$ and used as initial values for p_φ and p_r the ones provided by the adiabatic approximation (see Eqs. (4.6) and (4.13) below). The dashed circle in this plot indicates the radial coordinate location of the LSO defined by the conservative part of the dynamics, i.e. by the Hamiltonian $\widehat{H}(r, p_r, p_\varphi)$. More precisely this "$r$-LSO" is simply defined (for any ν) by $r = r_{\rm LSO}(\nu)$, where $r_{\rm LSO}(\nu)$ is the solution of

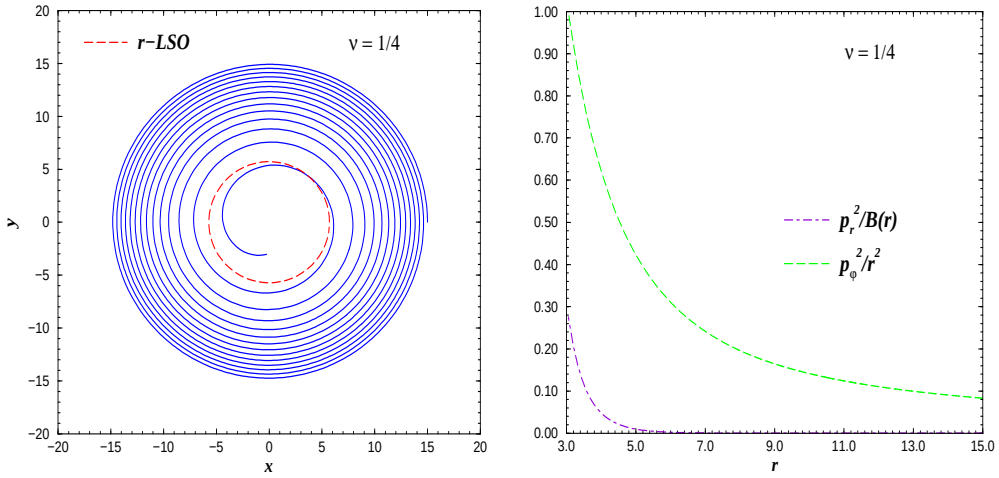

FIG. 1. *On the left panel we show the inspiraling circular (relative) orbit for* $\nu = 1/4$. *The location of the r-LSO, defined by the conservative part of the dynamics, is also indicated. On the right panel we compare the two kinetic contributions that enter the Hamiltonian: the "radial" and the "azimuthal" one. The figure shows that the assumption we made of quasi-circularity, i.e.* $p_r^2/B(r) \ll p_\varphi^2/r^2$, *is well satisfied throughout the transition from the adiabatic phase to the plunge.*

Eq. (2.17). In particular, $r_{\rm LSO}\left(\frac{1}{4}\right) = 5.718$, as recalled in Eq. (2.18). Note that, in presence of radiation reaction effects, there is an arbitrariness in what one would like to mean by saying: "the system is crossing the LSO". Indeed, we could define the "LSO-crossing" in several inequivalent ways, notably: (i) r-LSO: the time when $r = r_{\rm LSO}(\nu)$; (ii) j-LSO: the time when $p_\varphi \equiv j = j_{\rm LSO}(\nu)$; (iii) ω-LSO: the time when $d\varphi/d\hat{t} \equiv \widehat{\omega} = \widehat{\omega}_{\rm LSO}(\nu)$. [The "LSO" functions of ν being defined by solving Eq. (2.17); see Eq. (2.18).] This arbitrariness is not a problem. Our new evolution system (3.41)–(3.44) describes a smooth transition "through" the formally defined "old" LSO, and does not care about old definitions. In other words, when ν is finite, and especially when $\nu \simeq 1/4$ (which, one should remember, is expected to be an *accumulation point* of observed values of ν; see footnote 2 above) the smooth transition process blurs the notion of LSO. It is only for $\nu \ll 1$ (see below) that one recovers a sharp transition near the H-defined LSO. On the right panel of Fig. 1 we compare the two kinetic contributions to the Hamiltonian (3.45): the "azimuthal" contribution p_φ^2/r^2, and the "radial" contribution $p_r^2/B(r)$. One sees on this Figure that our basic assumption of quasi-circularity (which, at the level of $\widehat{H}$, means $p_r^2/B(r) \ll p_\varphi^2/r^2$) is well satisfied

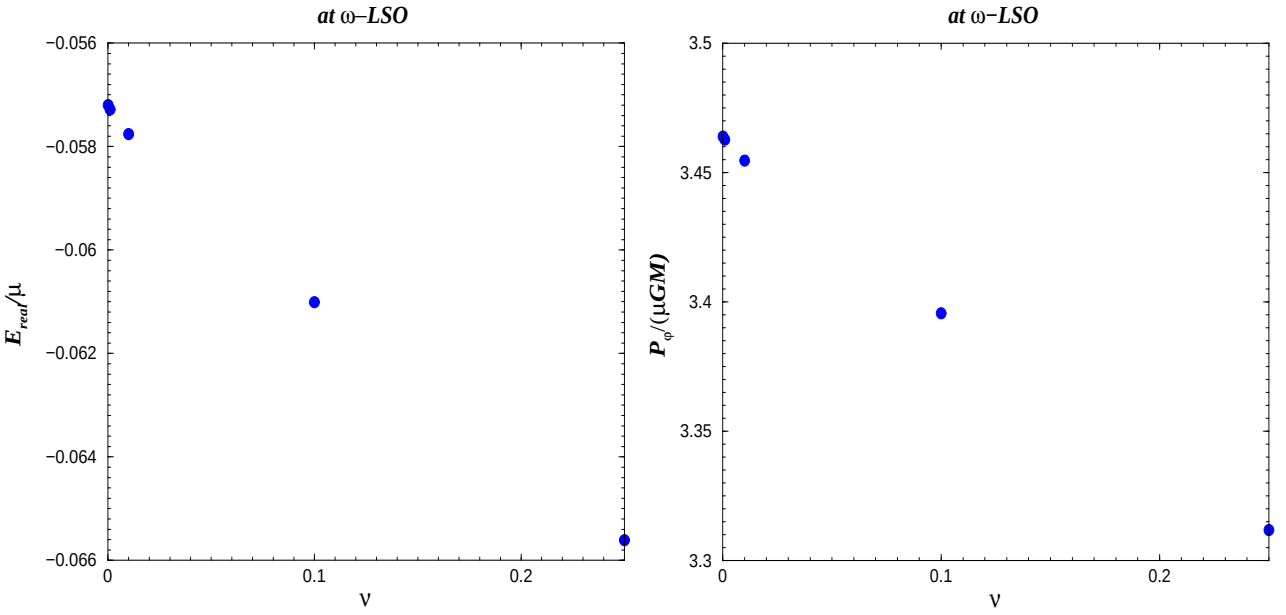

FIG. 2. *Variation with ν of the ω-LSO values of the real reduced non-relativistic energy $E^{\rm NR}_{\rm real}/\mu = (\mathcal{E}_{\rm real} - M)/\mu$ (on the left), and of the real angular momentum $j = P_\varphi/(\mu GM)$ (on the right), computed integrating the full dynamics, i.e. with radiation reaction effects included.*

throughout the transition. In fact, even down to $r \simeq 3.79$ one has $p_r^2/B(r) < 0.1\, p_\varphi^2/r^2$. The radial kinetic energy would become equal to the azimuthal one only below $r = 3$. We shall, anyway, not use, in the following, our system below the (usual) "light-ring" $r \simeq 3$ (where $p_r^2/B(r) \simeq 0.30\, p_\varphi^2/r^2$).

We exhibit more quantitative results on the transition between the inspiral and the plunge in Figs. 2 and 3. These figures plot the values of several physical quantities (energy, angular momentum, radial velocity and radial coordinate) computed at the ω-LSO (i.e. when $\omega = \omega_{\rm LSO}(\nu)$) after integration of the system (3.41)–(3.44). The energy which is plotted is the reduced non-relativistic real energy, i.e. $(\mathcal{E}_{\rm real} - M)/\mu$. [In the test-mass limit, this reduced energy equals $\sqrt{8/9} - 1 = -0.057191$.]

Having obtained, through Figs. 2 and 3, a first impression of the physics of the inspiral $\rightarrow$ plunge transition, we shall now study in more detail this transition, notably by comparing it with various analytical approximations. The first approximation we shall consider is the current standard one used for dealing with the inspiral phase: the adiabatic approximation.

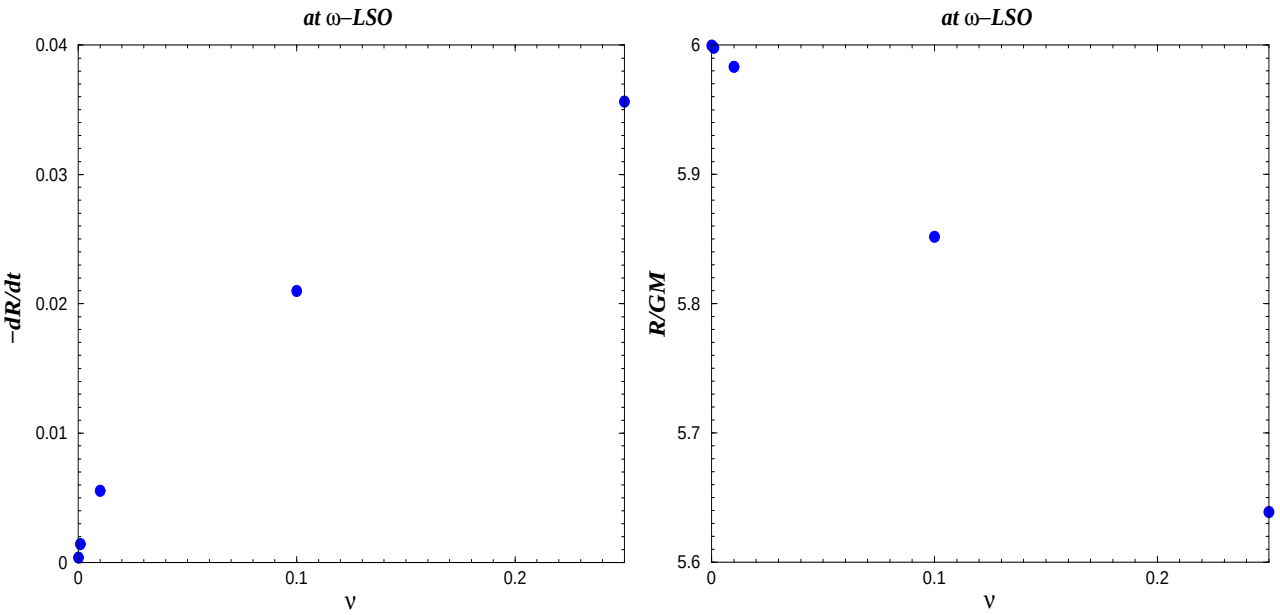

FIG. 3. *ω-LSO values of the radial velocity (on the left) and of the radial position (on the right) versus ν, derived integrating the full dynamical evolution.*

A. Comparison with the adiabatic approximation

Let us compare the exact numerical evolution with the usual adiabatic approximation to inspiral motion. This approximation is defined by saying that the (effective) body follows an adiabatic sequence of exact circular orbits whose energy is slowly drained out by gravitational radiation. It is obtained from Eqs. (3.41), (3.44), by neglecting p_r^2, i.e. by setting $p_r = 0$. Noticing that $\partial \widehat{H}/\partial p_r = 2p_r\, \partial \widehat{H}/\partial p_r^2 \propto p_r$ we get that $dr/d\hat{t}$ vanishes linearly with p_r. The first equation (3.41) is then formally satisfied with $p_r = 0 = \dot{r}$. Imposing now $p_r = 0$ in Eqs. (3.42) and (3.43) we obtain two further equations:

$$\frac{\partial \widehat{H}_0}{\partial r}(r, p_\varphi) = 0\,, \tag{4.1}$$

$$\widehat{\omega} = \frac{\partial \widehat{H}_0}{\partial p_\varphi}(r, p_\varphi)\,, \tag{4.2}$$

where we define

$$\widehat{H}_0(r, p_\varphi) \equiv \widehat{H}(r, p_r = 0, p_\varphi) = \frac{1}{\nu}\sqrt{1 + 2\nu\left[\sqrt{A(r)\left(1 + \frac{p_\varphi^2}{r^2}\right)} - 1\right]}\,. \tag{4.3}$$

Eq. (4.1) provides a link between r and $p_\varphi \equiv j$ in the adiabatic limit. From the structure (3.45) of $\widehat{H}$, it is easily seen that Eq. (4.1) is equivalent to looking for the minimum, say (for convenience) in the variable $u \equiv 1/r$, of the "radial potential"

$$W_j(u) = A(u)\,[1 + j^2\,u^2]\,. \tag{4.4}$$

Solving $\partial_u W_j(u) = 0$ gives a parametric representation of j^2 in terms of u:

$$j^2_{\rm adiab}(u) = -\frac{A'(u)}{(u^2\,A(u))'}\,, \tag{4.5}$$

where the prime denote d/du. In the case where the function A is given by Eq. (3.47), i.e. $A(u) = 1 - 2u + 2\nu\,u^3$, Eq. (4.5) yields, in term of the orignal (reduced) radial variable $r = 1/u$

$$j^2_{\rm adiab.}(r) = \frac{r^2\,(r^2 - 3\,\nu)}{r^3 - 3r^2 + 5\nu}\,. \tag{4.6}$$

Note that there exist real circular orbits (though possibly unstable ones) as long as $j^2_{\rm adiab}(r) > 0$, i.e. as long as $r^3 - 3r^2 + 5\nu > 0$. In fact the positive, real solution in r of

$$[r^3 - 3r^2 + 5\nu]_{\rm light-ring} = 0 \tag{4.7}$$

defines the light-ring or last unstable circular orbit (with $j^2(r_{\rm light-ring}) = +\infty$). We find $r_{\rm light-ring} \simeq 2.84563$ in the case $\nu = 1/4$. Eq. (4.2) then gives the parametric representation of $\widehat{\omega} = \omega\,(GM)$ throughout the adiabatic phase for circular orbits:

$$\widehat{\omega}_{\rm adiab.}(r) = \frac{1}{r^{3/2}}\,\frac{\sqrt{1 - 3\nu/r^2}}{\sqrt{1 + 2\nu(\sqrt{z(r)} - 1)}}\,, \tag{4.8}$$

where $z(r)$ denotes the following quantity

$$z(r) \equiv \widehat{H}^2_{\rm eff}(r, p_r = 0, p_\varphi = j_{\rm adiab.}) = \frac{r^3\,A^2(r)}{r^3 - 3\,r^2 + 5\nu}\,. \tag{4.9}$$

Note that the effective one-body description seems to become somewhat unsatisfactory at the light-ring (at least for exactly circular orbits). Indeed, we see from Eqs. (4.8) and (4.9) that the blow up of $z(r)$, i.e. of the effective energy, at the light-ring, Eq. (4.7), implies that the real orbital frequency of circular orbits, $\widehat{\omega}_{\rm circ.}(r)$, Eq. (4.8), tends to zero at the light-ring. This is probably an unphysical behaviour [from the test-mass limit, one expects

the orbital frequency to have a non-zero limit at the light-ring; see, e.g., Ref. [6] where Padé approximants are used to compute a finite value of $\widehat{\omega}_{\rm light-ring}(\nu)$]. The other factors in Eq. (4.8) imply, as expected, a regular *increase* of $\widehat{\omega}(r)$ as r decreases below the LSO. Pending the construction of an improved version of the effective one-body approach which would be better behaved, we have decided, when dealing with the evolution of the system (3.41)–(3.44), to stop the simulation at the light-ring. [In our simulations of plunging orbits the effective energy stays bounded, but the orbital frequency $\widehat{\omega}(\hat{t})$ levels off very close to the light-ring.]

Finally Eq. (3.44) becomes in the adiabatic limit

$$\frac{dj}{d\hat{t}} = \widehat{\mathcal{F}}_\varphi \left(\frac{\partial \widehat{H}_0}{\partial p_\varphi}(r,j) \right) . \tag{4.10}$$

Then using $dj/d\hat{t} = (dj/dr)\,(dr/d\hat{t})$ and $d\varphi = \widehat{\omega}\, d\hat{t}$ we can solve the motion in the adiabatic limit by quadratures:

$$d\hat{t}_{\rm adiab.} = \left(\frac{dj_{\rm adiab.}}{dr} \right) \frac{dr}{\widehat{\mathcal{F}}_\varphi(\widehat{\omega}_{\rm adiab.}(r))} , \tag{4.11}$$

$$d\varphi_{\rm adiab.} = \left(\frac{dj_{\rm adiab.}}{dr} \right) \frac{\widehat{\omega}_{\rm adiab.}(r)}{\widehat{\mathcal{F}}_\varphi(\widehat{\omega}_{\rm adiab.}(r))}\, dr . \tag{4.12}$$

The radial velocity $v_r \equiv dr/d\hat{t}$, as a function of the parameter r, in the adiabatic limit, is given by:

$$v_r^{\rm adiab.} = \frac{\widehat{\mathcal{F}}_\varphi(\widehat{\omega}_{\rm adiab.}(r))}{dj_{\rm adiab.}/dr} . \tag{4.13}$$

Note that $v_r^{\rm adiab.}$ formally tends to $-\infty$ when $r \to r_{\rm LSO}$ (indeed, $j_{\rm adiab.}(r)$ reaches, by definition, a minimum at $r = r_{\rm LSO}$). This shows that the adiabatic approximation is meaningful only during the inspiral phase (i.e. "above" the LSO). In Figs. 4, 5 we compare, for $\nu = 1/4$, the number of gravitational cycles, defined by $\mathcal{N}_{\rm GW} = \varphi_{\rm GW}/(2\,\pi) = \varphi/\pi$, the orbital angular frequency ω (or, equivalently, the gravitational wave frequency, $f_{\rm GW} = \omega_{\rm GW}/(2\pi) = \omega/\pi$), and the radial velocity, computed with the exact equations of motion and in the adiabatic limit, as well as the gravitational waveform. These figures show that, in the equal-mass case $\nu = 1/4$, the adiabatic approximation starts to significantly deviate from the exact evolution quite before one reaches the LSO. Fig. 4 is normalized so that $\mathcal{N}_{\rm GW}^{\rm adiab}$ and $\mathcal{N}_{\rm GW}^{\rm exact}$ coincide for

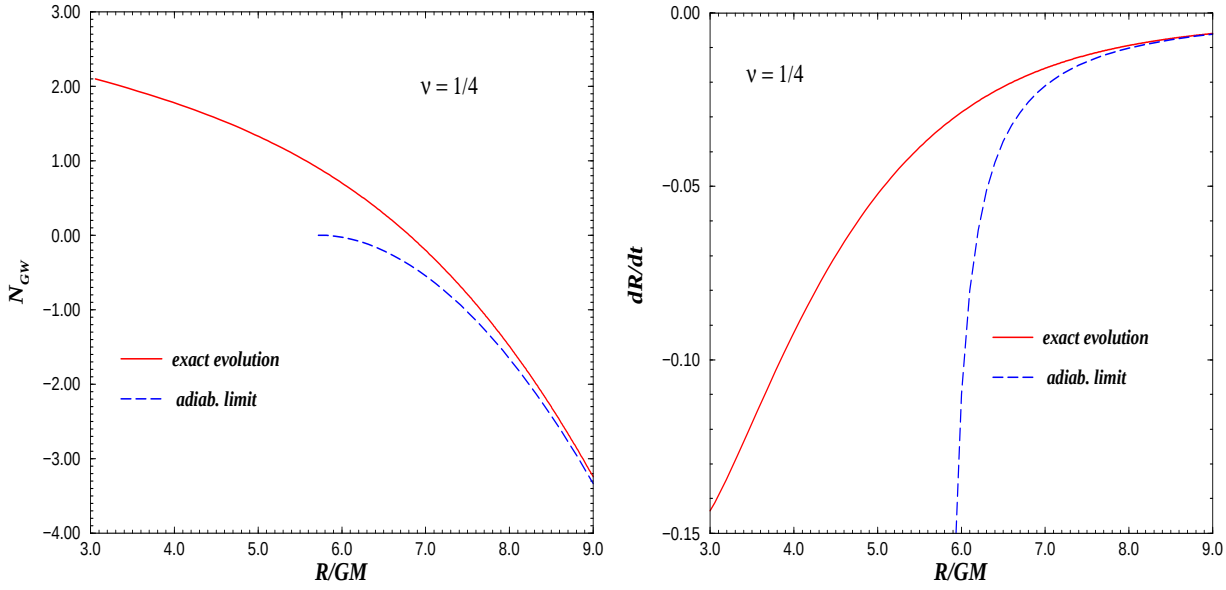

FIG. 4. *We compare the number of gravitational cycles (on the left) and the radial velocity (on the right), computed with the exact evolution and within the adiabatic approximation, versus* R/GM.

large values of R/GM, and that $\mathcal{N}^{\rm adiab}_{\rm GW}$ be zero at the r-LSO. For instance, we find that the number of GW cycles given by the adiabatic approximation differs from the exact number already by 0.1 when $r \simeq 8.8$, and that $\mathcal{N}^{\rm exact}_{\rm GW}(r_{\rm LSO}) = 0.9013$. The left panel of Fig. 5 contrasts $\omega/\omega_{\rm LSO}$ $(= f_{\rm GW}/f^{\rm Schw.}_{\rm GW\,LSO}$ where $f^{\rm Schw.}_{\rm GW\,LSO} = 6^{-3/2}/GM\pi$ is the fiducial Schwarzschild LSO GW frequency), computed with the exact evolution and within the adiabatic approximation, as a function of time. Note that, for the horizontal axis we use $\widehat{\omega}_{\rm LSO}(0)(\hat{t} - \hat{t}_{\rm LSO})$, where $\widehat{\omega}_{\rm LSO}(0) = \pi \widehat{f}^{\rm Schw.}_{\rm GW\,LSO} = 6^{-3/2}$ (provided by the $\nu \to 0$ limit of Eq. (2.19)) and $\hat{t}_{\rm LSO}$ is defined as the time at which the adiabatic solution reaches the r-LSO position. Finally, on the right panel of Fig. 5 we compare the last few GW cycles of the exact and the adiabatic *restricted* waveform, i.e. $h(t) \equiv v^2 \cos \phi_{\rm GW}(t)$, with $v = (d\varphi/d\hat{t}\,)^{1/3}$ and $\phi_{\rm GW} = 2\varphi$, in the crucial interesting region around the LSO. By *adiabatic* restricted waveform we mean the restricted waveform in which $\varphi(\hat{t}) = \varphi_{\rm adiab.}(\hat{t})$ is derived by integrating the two equations (4.11) and (4.12) (which give a parametric representation of $\hat{t}_{\rm adiab.}(r)$ and $\widehat{\varphi}_{\rm adiab.}(r)$ in terms of the auxiliary parameter r).

Note in Fig. 5 that the dephasing between the two waveforms becomes visible somewhat

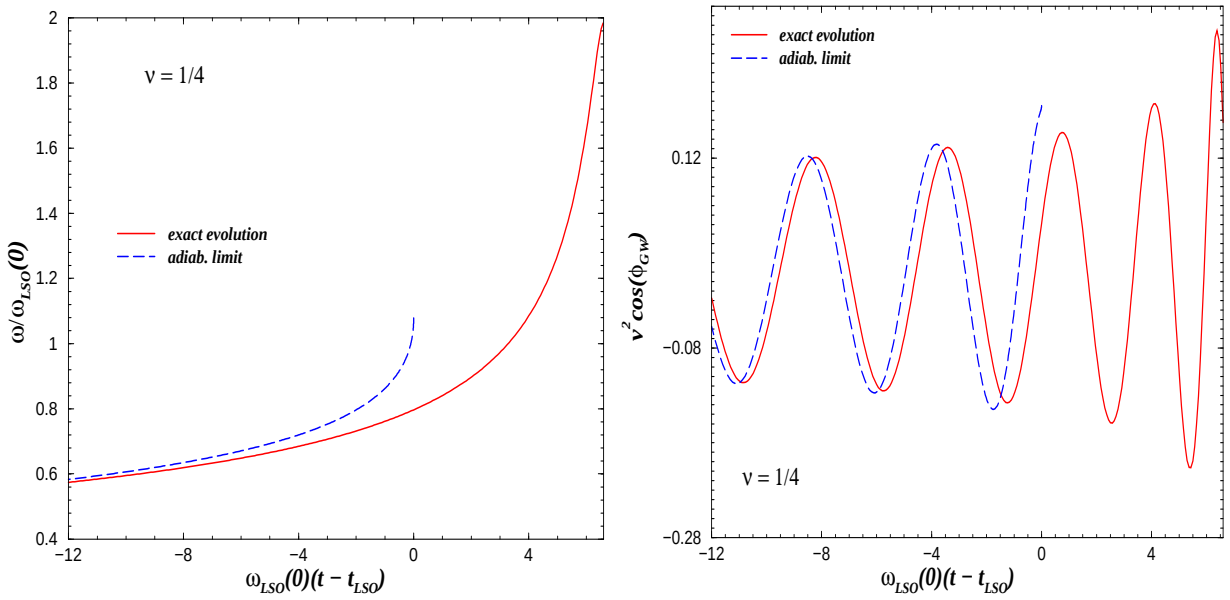

FIG. 5. *We contrast the orbital frequency (on the left), divided by the Schwarzschild value* $\widehat{\omega}_{\rm LSO}(0) = 6^{-3/2}$*, and the restricted waveform (on the right), evaluated with the exact dynamical system and within the adiabatic approximation. Note that in both plots the quantities are given as a function of the rescaled time variable* $\widehat{\omega}_{\rm LSO}(0)(\hat{t} - \hat{t}_{\rm LSO})$*, where* $\hat{t}_{\rm LSO}$ *is defined as the time at which the adiabatic solution reaches the r-LSO position.*

before the LSO (we shall dwell more on this subject in Section V). Note also that the time when the adiabatic evolution reaches the LSO ("adiabatic LSO") corresponds to a time when the exact evolution reaches a frequency $\omega \simeq 0.80\,\omega_{\rm LSO}(0)$, i.e. a time significantly *before* the ω-LSO. This is why there are more cycles after the adiabatic LSO in Fig. 5 (more than two cycles), than there will be after the (exact) ω-LSO (we shall see below that $N_{\rm GW}^{\rm afterLSO} = 2N_{\rm orbit}^{\rm afterLSO} = 1.2048$ for $\nu = 1/4$).

B. The $\dot{r}$-linearized approximation

The previous subsection has shown the severe shortcomings of the adiabatic approximation. Let us now consider a second analytical approximation which is more accurate than the adiabatic one, and which, in particular, allows one to see analytically what happens during the transition between the inspiral and the plunge. This approximation is based on a simple

linearization with respect to the radial velocity $dr/d\hat{t}$, which is small during the inspiral, as well as the beginning of the plunge.

As $\widehat{H}$ depends quadratically on p_r and $p_r \ll 1$ we pose

$$C_r(r,j) \equiv \left[\frac{1}{p_r}\frac{\partial \widehat{H}}{\partial p_r}(r,p_r,j)\right]_{p_r\to 0} = \frac{1}{\nu\,\widehat{H}_0(r,j)}\,\frac{1}{\widehat{H}^0_{\rm eff}(r,j)}\,\frac{A^2(r)}{1-6\nu/r^2}\,, \tag{4.14}$$

(note that C_r is a positive quantity), where

$$\widehat{H}^0_{\rm eff}(r,j) = \widehat{H}_{\rm eff}(r,p_r=0,j) = \sqrt{A(r)\,\left(1+\frac{j^2}{r^2}\right)}\,. \tag{4.15}$$

Then, modulo p_r^2 fractional effects that we neglect, we can write

$$\frac{dr}{d\hat{t}} \simeq C_r(r,j)\,p_r\,. \tag{4.16}$$

Differentiating twice the above equation with respect to time, we obtain

$$\frac{d^2p_r}{d\hat{t}^2} \simeq \frac{1}{C_r(r,j)}\,\frac{d^3r}{d\hat{t}^3}\,, \tag{4.17}$$

when neglecting some nonlinear terms $\propto (dr/d\hat{t})^2$ and $(dr/d\hat{t})\,(dj/d\hat{t})$. On the other hand, taking the derivative with respect to time of Eq. (3.43) and neglecting fractional corrections of $\mathcal{O}(p_r^2)$, we end up with

$$\frac{d^2p_r}{d\hat{t}^2} = -\frac{d}{d\hat{t}}\,\frac{\partial \widehat{H}}{\partial r}(r,p_r,p_\varphi) \simeq -\frac{\partial^2 \widehat{H}_0}{\partial r^2}\,\frac{dr}{d\hat{t}} - \frac{\partial^2 \widehat{H}_0}{\partial r \partial j}\,\widehat{\mathcal{F}}_\varphi\,. \tag{4.18}$$

To get an autonomous system we further approximate j by solving for j in the lowest-order approximation to Eq. (3.43), obtained by neglecting both p_r and $dp_r/d\hat{t}$. In other words, $j(r)$ is obtained, as in adiabatic approximation, by solving Eq. (4.1). Finally, $j \simeq j_{\rm adiab.}(r)$, as given by Eq. (4.6). We define

$$\begin{aligned}\omega_r^2(r) &\equiv C_r(r,j_{\rm adiab.}(r))\,\frac{\partial^2 \widehat{H}_0}{\partial r^2}(r,j_{\rm adiab.}(r))\,,\\ &= \frac{1}{\nu^2\,\widehat{H}_0^2(r,j_{\rm adiab.})}\,\frac{r^5-6\,r^4+3\nu\,r^3+20\nu\,r^2-30\,\nu^2}{r^6\,(r^2-6\nu)}\,,\end{aligned} \tag{4.19}$$

$$\begin{aligned}B_r(r) &\equiv C_r(r,j_{\rm adiab.}(r))\,\frac{\partial^2 \widehat{H}_0}{\partial r \partial j}(r,j_{\rm adiab.}(r))\,\widehat{\mathcal{F}}_\varphi(\widehat{\omega}_{\rm adiab.}(r))\,,\\ &= -\frac{2\,j_{\rm adiab.}(r)}{\nu^2\,\widehat{H}_0^2(r,j_{\rm adiab.})}\,\frac{(r^3-3r^2+5\nu)^2}{r^7\,(r^2-6\nu)}\,\widehat{\mathcal{F}}_\varphi(\widehat{\omega}_{\rm adiab.}(r))\,,\end{aligned} \tag{4.20}$$

(where the replacements $j \to j_{\rm adiab.}(r)$ are done after the partial differentiations). It is easily seen that the quantity $\partial^2 \widehat{H}_0 / \partial r \, \partial j$ is negative, so that ($\widehat{\mathcal{F}}_\varphi$ being also negative) the quantity B_r given by Eq. (4.20) is positive.

Combining Eqs. (4.17) and (4.18), we finally derive the following third order differential equation in r:

$$\frac{d^3 r}{d\hat{t}^3} + \omega_r^2(r) \, \frac{dr}{d\hat{t}} \simeq -B_r(r) \, . \tag{4.21}$$

We shall often refer to Eq. (4.21) as the "linear $\dot{r}$-equation" because it was obtained by working linearly in the radial velocity $\dot{r} = dr/d\hat{t}$. [Note, however, that this is a third-order *nonlinear* differential equation in r.] It is easily seen that the quantity $\omega_r^2(r)$ defines the square of the frequency of the radial oscillations. As seen in Eq. (4.19) it is proportional to the curvature of the effective radial potential $H_0(r, j)$ determining the radial motion. Above the LSO, i.e. when $r > r_{\rm LSO}(\nu)$, the radial potential has a *minimum* (defining the stable circular orbit with angular momentum j) and, therefore, $\omega_r^2(r)$ is positive. When $r = r_{\rm LSO}(\nu)$, the radial potential has an inflection point (see Eq. (2.17)), and, therefore, $\omega_r^2(r)$ vanishes. When $r < r_{\rm LSO}(\nu)$, the radial potential is concave, and $\omega_r^2(r)$ becomes negative. [See, e.g., Fig. 1 of [7] for a plot of the shape of the radial potential.]

Within the same approximation used above (i.e., essentially, neglecting terms which are *fractionally* of order p_r^2), we can finally write the angular frequency along our quasi-circular orbits as

$$\frac{d\varphi}{d\hat{t}} \simeq \frac{\partial \widehat{H}_0}{\partial j} \left(r, j_{\rm adiab.}(r) \right) . \tag{4.22}$$

Note that φ is obtained from this equation by a quadrature, once the radial motion $r(\hat{t})$ is known from the integration of Eq. (4.21).

The conceptually interesting feature of the above "$\dot{r}$-linearized" approximation is the structure of Eq. (4.21). The previously considered "adiabatic" approximation corresponds to neglecting $d^3 r / d\hat{t}^3$ in Eq. (4.21). We now see that this is a good approximation only when the characteristic frequency of variation of the radial motion, defined, say, by $\omega^2_{\rm caract.} \equiv (d^3 r / d\hat{t}^3)/(dr/d\hat{t})$ is much smaller than the frequency of radial oscillations ω_r^2 (determined by the restoring radial force ensuring the existence of stable circular orbits). As ω_r^2 tends to zero, before changing sign, at the LSO, it is clear that the adiabatic approximation must break down somewhat above the LSO. When it breaks down the "inertia term" $d^3 r / d\hat{t}^3$ in

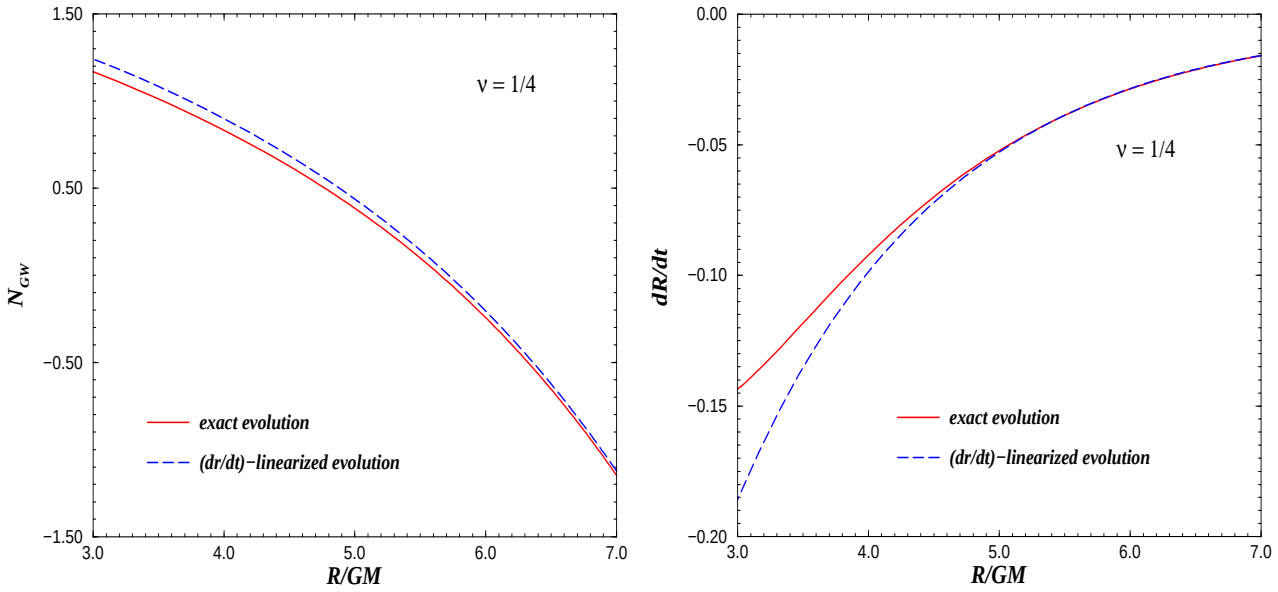

FIG. 6. *Contrast of the number of gravitational cycles (on the left) and the radial velocity (on the right), computed with the exact evolution and the linear-$\dot{r}$ equation, versus R/GM.*

Eq. (4.21) becomes comparable to both the "restoring force" term $\omega_r^2\, dr/d\hat{t}$ and the "driving force" $-B_r$ coming from gravitational radiation damping.

In Figs. 6 we compare the number of gravitational cycles and the radial velocity evaluated with the exact evolution and the $\dot{r}$-linearized equations. We start the evolution at $r = 15$ and fix the initial values of $dr/d\hat{t}$ and $d^2r/d\hat{t}^2$ in the "adiabatic approximation" defined by neglecting in Eq. (4.21) the "inertia term" $d^3r/d\hat{t}^3$ (and then by differentiating again the resulting approximate equation). Moreover, we normalize $\mathcal{N}_{\rm GW}^{\rm linear}$ to be zero at the r-LSO. We derive from the exact evolution $\mathcal{N}_{\rm GW}^{\rm exact}(r_{\rm LSO}) = -0.04223$. The main conclusion drawn from Figs. 6 is that the $\dot{r}$-linearized approximation is quite good both during the inspiral phase and, more importantly, during the transition to the plunge taking place near the LSO. This is interesting to know because it shows that the crucial physical effect that is lacking in the usually considered adiabatic approximation is the simple "inertia term" $d^3r/d\hat{t}^3$ in Eq. (4.21). Note, however, that in order to add this inertia term it is necessary to have in hand the Hamiltonian describing at least the slightly non-circular orbits (the normalization of Eq. (4.21) crucially depends on the knowledge of ω_r^2 which depends both on $\partial\widehat{H}/\partial p_r^2$

and on $\partial^2 \widehat{H}/\partial r^2$). This being said, we do not, however, recommend to use in practice the $\dot{r}$-linearized approximation. Indeed, we think that the "exact" system (3.41)–(3.44) is a more accurate description of the evolution of the system because it keeps all the nonlinear effects in p_r^2. Numerically speaking, it is essentially as easy to integrate the "exact" system than its $\dot{r}$-linearized approximation, so that there would be anyway no practical advantage in downgrading the accuracy of the system (3.41)–(3.44). However, we shall see next that the $\dot{r}$-linearized system can be further used to lead to a simple analytical approach to the transition to the plunge in the case where $\nu \ll 1$.

C. The universal ρ-equation

Until now we have been considering the general case where the symmetric mass ratio $\nu \equiv m_1 m_2/(m_1+m_2)^2$ can be of order of its maximum value $\nu_{\max} = 1/4$. As is clear from the results above when 4ν is of order unity the *non-adiabatic* aspects of radiation damping effects become important in an extended region of order $\Delta(R/GM) \sim 1$, above the standard LSO. On the other hand, we expect that when $4\nu \ll 1$ the transition between the adiabatic inspiral and the plunge will be sharply localized around the standard LSO, defined by Eq. (2.17). Indeed, when ν is a small parameter, the damping force $\widehat{\mathcal{F}}_\varphi$, Eq. (3.46), being proportional to ν, can be treated as a perturbatively small quantity in the evolution of the system. Consequently, the "driving force" term, $-B_r$, in the $\dot{r}$-linearized equation (4.21) contains the small parameter ν. It is then clear that all the time derivatives of r (being driven by B_r) will tend to zero with ν. If the coefficient ω_r^2 in Eq. (4.21) never vanishes it is easy to see how one would satisfy Eq. (4.21) by solving for $dr/d\hat{t}$, while considering $d^3r/d\hat{t}^3$ as a fractionally small term (to be evaluated by further differentiating $dr/d\hat{t} \simeq -B_r/\omega_r^2$). In that case, one sees that $dr/d\hat{t}$ would be $\mathcal{O}(\nu)$ (and $d^3r/d\hat{t}^3 = \mathcal{O}(\nu^3)$) as $\nu \to 0$. However, the fact that $\omega_r^2(r)$ vanishes when $r = r_{\rm LSO}(\nu)$ shows that the way $dr/d\hat{t}$ tends to zero with ν, near the LSO, is more subtle. Having understood from this reasoning that, when $\nu \to 0$, the interesting transition effects take place very near the LSO, we now turn to a precise analysis of this transition.

A first method for dealing (when $\nu \to 0$) with this transition would be (as just sketched) to continue working with the third-order equation (4.21), considered in the immediate neighbourhood of $r = r_{\rm LSO}(\nu)$. However, it is better (in order not to increase the differential order)

to go back to the exact system (3.41)–(3.44) and to approximate it directly when $\nu \to 0$ and $r \to r_{\rm LSO}(\nu)$.

Let us see the consequences of the evolution (3.41)–(3.44) when r is very near $r_{\rm LSO}(\nu)$. To do this it is convenient to introduce some notation. Using, as we did in Sec. IV B, the fact that $\widehat{H}$ depends quadratically on p_r and that $p_r \ll 1$, we define:

$$C_r^{\rm LSO}(\nu) \equiv \left[\frac{1}{p_r} \frac{\partial \widehat{H}}{\partial p_r}(r, p_r, j) \right]_{p_r \to 0}^{\rm LSO} . \tag{4.23}$$

Note that $C_r^{\rm LSO}$ is a number, which depends on ν [5]. In terms of the previous definition (4.14), one has simply $C_r^{\rm LSO}(\nu) = C_r(r_{\rm LSO}(\nu), j_{\rm LSO}(\nu))$. Explicitly, it reads

$$C_r^{\rm LSO}(\nu) = \left[\frac{A^2(r)}{\nu\, \widehat{H}_0(r,j)\, \widehat{H}^0_{\rm eff}(r,j)\, (1 - 6\nu/r^2)} \right]_{\rm LSO} . \tag{4.24}$$

In the $\nu = 0$ limit this simplifies to

$$C_r^{\rm LSO}(0) = \frac{\sqrt{2}}{3} . \tag{4.25}$$

The point in having introduced the notation (4.23) is that Eq. (3.41) reads simply, when one is very near the LSO:

$$p_r \simeq \frac{1}{C_r^{\rm LSO}} \frac{dr}{d\hat{t}} . \tag{4.26}$$

This allows us to recast Eq. (3.43) in the form (after neglecting fractional p_r^2 terms on the RHS)

$$\frac{1}{C_r^{\rm LSO}} \frac{d^2 r}{d\hat{t}^2} \simeq - \frac{\partial \widehat{H}_0}{\partial r}(r, j) . \tag{4.27}$$

Here, as above, $\widehat{H}_0(r,j) \equiv \widehat{H}(r, p_r = 0, p_\varphi \equiv j)$. Then we expand the RHS of the above equation around the LSO, i.e. we write

---

[5] As we consider $\nu \ll 1$, we could further take the limit $\nu \to 0$ in all the quantities which have a finite limit as $\nu = 0$. However, in order not to unnecessarily loose accuracy we shall not do so. For instance we shall always consider that $r_{\rm LSO}(\nu)$ is computed for $\nu \neq 0$, though we shall see later that the direct ν-dependence in $r_{\rm LSO}(\nu)$ (which is $\mathcal{O}(\nu)$) is parametrically small compared to the width $\mathcal{O}(\nu^{2/5})$ of the radial axis where the transition takes place.

$$r = r_{\rm LSO}(\nu) + \delta r\,, \qquad j = j_{\rm LSO}(\nu) + \delta j\,. \tag{4.28}$$

Keeping the first nontrivial terms in the expansion in powers of δr and δj (and neglecting subleading terms, such as those of order $\mathcal{O}(\delta r \delta j)$, $\mathcal{O}((\delta j)^2)$ and $\mathcal{O}((\delta r)^3)$) one obtains

$$\frac{\partial \widehat{H}_0}{\partial r} \simeq \frac{1}{2}\left(\frac{\partial^3 \widehat{H}_0}{\partial r^3}\right)_{\rm LSO} (\delta r)^2 + \left(\frac{\partial^2 \widehat{H}_0}{\partial r \partial j}\right)_{\rm LSO} (\delta j)\,. \tag{4.29}$$

Moreover, near the LSO we can write Eq. (3.44) as:

$$\frac{d(\delta j)}{d\hat{t}} = \frac{dj}{d\hat{t}} \simeq \widehat{\mathcal{F}}_\varphi(\widehat{\omega}_{\rm LSO})\,, \qquad \text{with} \quad \widehat{\omega}_{\rm LSO} = \left(\frac{\partial \widehat{H}_0}{\partial j}\right)_{\rm LSO}\,. \tag{4.30}$$

This yields

$$\delta j \simeq \widehat{\mathcal{F}}_\varphi(\widehat{\omega}_{\rm LSO})\,(\hat{t} - \hat{t}_{\rm LSO})\,, \tag{4.31}$$

where $\hat{t}_{\rm LSO}$ is the time at which $j(\hat{t}) = j_{\rm LSO}(\nu)$. Let us also define

$$A_r^{\rm LSO} \equiv C_r^{\rm LSO}\left(\frac{\partial^3 \widehat{H}_0}{\partial r^3}\right)_{\rm LSO}\,, \qquad B_r^{\rm LSO} \equiv C_r^{\rm LSO}\left(\frac{\partial^2 \widehat{H}_0}{\partial r \partial j}\right)_{\rm LSO} \widehat{\mathcal{F}}_\varphi(\widehat{\omega}_{\rm LSO})\,. \tag{4.32}$$

The quantity $B_r^{\rm LSO}$ is the LSO value of the quantity $B_r(r)$ introduced in Eq. (4.20) above. The explicit values of these quantities are

$$\begin{aligned} A_r^{\rm LSO}(\nu) &= \left[\frac{(r^3 - 2\,r^2 + 2\nu)\,(-210\nu\,j^2 - 60\nu\,r^2 + 60 j^2\,r^2 - 12 j^2\,r^3 + 6 r^4)}{r^7\,(r^2 - 6\nu)\,(j^2 + r^2)\,\nu^2\,\widehat{H}_0^2(r,j)}\right]_{\rm LSO}\,, \\ B_r^{\rm LSO}(\nu) &= \left[-\frac{2j\,(r^3 - 2r^2 + 2\nu)\,(r^3 - 3r^2 + 5\nu)}{r^5\,(r^2 - 6\nu)\,(r^2 + j^2)\,\nu^2\,\widehat{H}_0^2(r,j)}\right]_{\rm LSO} \widehat{\mathcal{F}}_\varphi(\widehat{\omega}_{\rm LSO})\,. \end{aligned} \tag{4.33}$$

In the $\nu = 0$ limit they simplify to

$$A_r^{\rm LSO}(0) = \frac{1}{1296}\,, \qquad B_r^{\rm LSO}(\nu) \overset{\nu\to 0}{=} -\frac{1}{72\sqrt{3}}\,\nu\left[\frac{\widehat{\mathcal{F}}_\varphi(\widehat{\omega}_{\rm LSO}(\nu);\nu)}{\nu}\right]_{\nu\to 0} = 1.052\cdot 10^{-4}\,\nu\,. \tag{4.34}$$

Finally, inserting Eq. (4.31) into Eq. (4.29), and replacing everything in Eq. (4.27) yields the simple equation

$$\frac{d^2\delta r}{d\hat{t}^2} + \frac{1}{2}\,A_r^{\rm LSO}\,(\delta r)^2 = -B_r^{\rm LSO}\,(\hat{t} - \hat{t}_{\rm LSO})\,. \tag{4.35}$$

This equation can be recast in a universal form by re-scaling the variables δr and $\delta\hat{t} = (\hat{t} - \hat{t}_{\rm LSO})$. Indeed, posing

$$\delta r = k_r\,\rho\,, \qquad \hat{t} - \hat{t}_{\rm LSO} = \delta\hat{t} = k_t\,\tau\,, \tag{4.36}$$

with

$$k_r \equiv (B_r^{\rm LSO})^{2/5}\,(A_r^{\rm LSO})^{-3/5}\,, \qquad k_t \equiv (A_r^{\rm LSO}\,B_r^{\rm LSO})^{-1/5}\,, \tag{4.37}$$

it is straightforward to derive the following "universal ρ-equation"

$$\frac{d^2\rho}{d\tau^2} + \frac{1}{2}\,\rho^2 = -\tau\,. \tag{4.38}$$

The explicit values of the scaling coefficients k_r and k_t are easily derived from our previous results. Let us only quote explicitly their $\nu = 0$ limit:

$$k_r(0) = 1.890\,\nu^{2/5}\,, \qquad k_t(0) = 26.19\,\nu^{-1/5}\,. \tag{4.39}$$

Note the interesting fractional scalings $k_r \propto \nu^{2/5}$, $k_t \propto \nu^{-1/5}$.

Let us also note the autonomous (time-independent) equation obtained by taking the time derivative of Eq. (4.38):

$$\frac{d^3\rho}{d\tau^3} + \rho\,\frac{d\rho}{d\tau} = -1\,. \tag{4.40}$$

Eq. (4.40) could have been directly derived by considering the $\dot{r}$-linearized Eq. (4.21) close to $r = r_{\rm LSO}$. There is, however, more information in Eq. (4.38) because its derivation showed that $\tau = 0$ marks the moment where $j(t) = j_{\rm LSO}(\nu)$.

The adiabatic approximation is recovered by neglecting in Eq. (4.38) the first term on the RHS. This gives

$$\rho_{\rm adiab.} = \sqrt{-2\tau}\,, \qquad \left(\frac{d\rho}{d\tau}\right)_{\rm adiab.} = -\frac{1}{\sqrt{-2\tau}} = -\frac{1}{\rho_{\rm adiab.}}\,. \tag{4.41}$$

The universal ρ and $\dot{\rho}$ curves and their adiabatic approximations are shown in Fig. 7. We have integrated Eq. (4.38) fixing the initial values (for large, negative τ) of ρ and $d\rho/d\tau$ in the adiabatic limit provided by Eq. (4.41). We see from Fig. 7 that the adiabatic approximation begins to be unacceptably bad when $\tau \simeq -1$. From the integration of Eq. (4.38) we get the important numerical values:

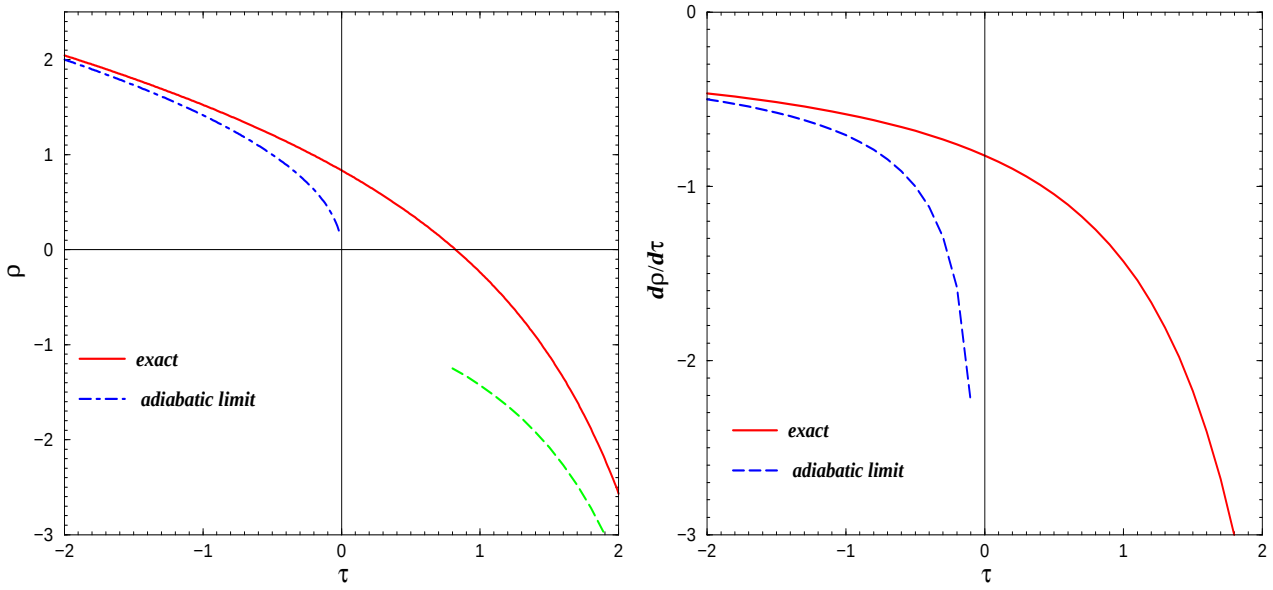

FIG. 7. *The universal ρ and $\dot{\rho}$ curves and their adiabatic approximations. The long-dashed curve at the bottom of the left panel represents the approximate asymptotic solution (4.53).*

$$\tau = 0: \quad \rho = 0.8339\,, \qquad \frac{d\rho}{d\tau} = -0.8233\,, \tag{4.42}$$

$$\rho = 0: \quad \tau = 0.8226\,, \qquad \frac{d\rho}{d\tau} = -1.267\,. \tag{4.43}$$

We recall that $\tau = 0$ marks the moment where $j(t) = j_{\rm LSO}(\nu)$, while $\rho = 0$ corresponds to $r(t) = r_{\rm LSO}$. The values given by Eqs. (4.42) and (4.43) can then be used to compute corresponding values of the physical quantities r, $dr/d\hat{t}$ and j by using the following parametric representations derived from our treatment above:

$$r(\tau) = r_{\rm LSO}(\nu) + k_r\,\rho(\tau)\,, \qquad \hat{t}(\tau) = \hat{t}_{\rm LSO} + k_t\,\tau\,, \tag{4.44}$$

$$j(\tau) = j_{\rm LSO}(\nu) + \widehat{\mathcal{F}}_\varphi(\widehat{\omega}_{\rm LSO})\,k_t\,\tau\,, \qquad \left(\frac{dr}{d\hat{t}}\right)(\tau) = \frac{k_r}{k_t}\,\frac{d\rho}{d\tau}\,. \tag{4.45}$$

Correspondingly to these approximate results for r, $\hat{t}$, j and $dr/d\hat{t}$, one can also write an approximate result for the angular frequency, namely

$$\begin{aligned}\left(\frac{d\varphi}{d\hat{t}}\right)(\tau) = \widehat{\omega}(\tau) &= \frac{\partial \widehat{H}_0}{\partial j}\,(r(\tau), j(\tau)) \\ &\simeq \widehat{\omega}_{\rm LSO}(\nu) + \left(\frac{\partial^2 \widehat{H}_0}{\partial r\,\partial j}\right)_{\rm LSO} k_r\,\rho(\tau) + \left(\frac{\partial^2 \widehat{H}_0}{\partial j^2}\right)_{\rm LSO} \widehat{\mathcal{F}}_\varphi^{\rm LSO}\,k_t\,\tau\,.\end{aligned} \tag{4.46}$$

In the approximation where we replace ν by zero in all quantities which have a finite limit when $\nu \to 0$, the above parametric results give the following explicit numerical links [except for $\hat{t}_{\rm LSO}$ which is an arbitrary integration constant]

$$r(\tau) = 6 + 1.890\,\nu^{2/5}\,\rho(\tau) + \mathcal{O}(\nu)\,, \qquad \hat{t}(\tau) = \hat{t}_{\rm LSO} + 26.19\,\nu^{-1/5}\,\tau\,, \tag{4.47}$$

$$j(\tau) = \sqrt{12} - 0.3436\,\nu^{4/5}\,\tau + \mathcal{O}(\nu)\,, \qquad \left(\frac{dr}{d\hat{t}}\right)(\tau) \simeq 0.07216\,\nu^{3/5}\,\frac{d\rho}{d\tau}\,, \tag{4.48}$$

$$\widehat{\omega}(\tau) = \frac{1}{6\sqrt{6}} - 0.03214\,\nu^{2/5}\,\rho(\tau) - 0.005062\,\nu^{4/5}\,\tau + \mathcal{O}(\nu)\,. \tag{4.49}$$

Note that these explicit results are less accurate than our previous implicit expressions Eqs. (4.44)–(4.45) (because of the $\mathcal{O}(\nu)$ error terms entailed by $r_{\rm LSO}(\nu) = r_{\rm LSO}(0) + \mathcal{O}(\nu)$, etc.). For consistency with the rest of the paper, we have used here (as in Eq. (4.34)) the $\nu \to 0$ limit of the value of $\nu^{-1}\,\mathcal{F}_\varphi^{\rm LSO}$ defined by the 2.5PN Padé estimate (3.46), namely $\nu^{-1}\,\mathcal{F}_\varphi^{\rm LSO} \simeq -0.01312$. Note that a more accurate value of this quantity is, according to Poisson's numerical results [25] $\nu^{-1}\,\widehat{\mathcal{F}}_\varphi^{\rm LSO} \simeq -0.01376$, which is $\simeq 5\%$ larger (in modulus). Note the various scalings with ν implied (when considering a point in the transition region parametrized by some fixed numerical values of ρ and τ) by Eqs. (4.44)–(4.45): notably $\delta r = \mathcal{O}(\nu^{2/5})$, $\delta j = \mathcal{O}(\nu^{4/5})$ and $p_r \sim \dot{r} = \mathcal{O}(\nu^{3/5})$. We shall discuss below in more details some of these scalings.

Fig. 7 vividly illustrates the fact (mentioned above) that the definition of "LSO-crossing" becomes ambiguous in presence of radiation damping. Indeed, for instance, the time where $r = r_{\rm LSO}(\nu)$ ("r-LSO"), i.e. the time where $\rho = 0$, differs from the time where $j = j_{\rm LSO}(\nu)$ ("j-LSO"), i.e. the time where $\tau = 0$ (see also Eq. (4.42)). An important issue is the domain of validity of the universal ρ-equation, i.e. the range of values of ν for which one can use Eqs. (4.44)–(4.45) to approximate the transition between inspiral and plunge. We have investigated this question numerically by comparing the radial velocity computed with the "exact" evolution (3.41)–(3.44), and with the ρ-equation (4.38). Let us define the practical limit of the domain of validity of the ρ-approximation by requiring that the fractional error in $dr/d\hat{t}$ at the (say) r-LSO be 10%. We find that this limit is reached when ν gets as large as

$$\nu_{\rm max} \simeq 0.05\,. \tag{4.50}$$

Therefore, the explicit expressions above can be used to estimate numerically the physical quantities in the transition region only for $\nu \leq \nu_{\rm max}$. Note that the accuracy of the ρ-results

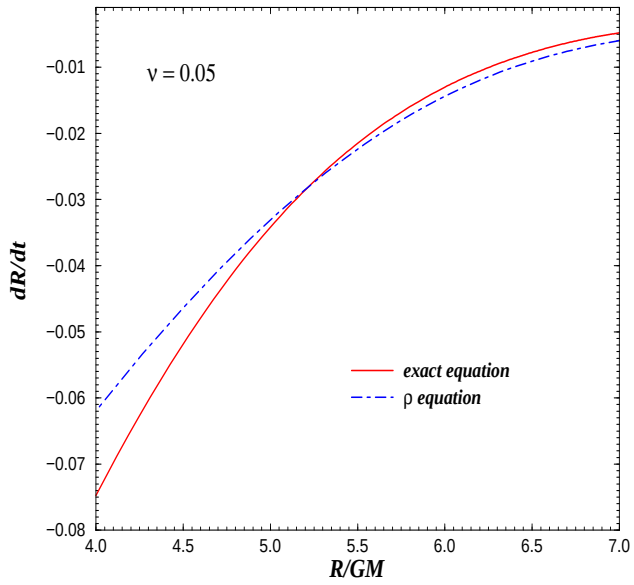

FIG. 8. *Plot of the radial velocity computed both with the exact evolution and with the ρ-equation in the case $\nu = 0.05$. The fractional error in dR/dt at the r-LSO is $\simeq 10\%$.*

above is, by construction, limited to some small neighbourhood of the LSO. They should not be used (even if $\nu < \nu_{\rm max}$) to estimate, for instance, the radial velocity at a radius which is significantly different from $r_{\rm LSO}$ (say at $r = 5$ or $r = 7$). To illustrate this we compare in Figs. 8 and 9 the radial velocity computed with the exact evolution, with that deduced from the ρ-equation. We examine three cases: $\nu = \nu_{\rm max} = 0.05$, $\nu = 10^{-2}$ and $\nu = 10^{-4}$.

Note that, though the accuracy of the approximation defined by the ρ-equation increases as $\nu \to 0$, its domain of validity actually shrinks as ν gets small. Indeed, if we keep ρ finite we see that $\delta r \simeq 1.890\, \nu^{2/5}\, \rho$, tends to zero with ν.

Before discussing the scaling predictions made by the ρ-approximation, let us comment on the various possible definitions of "LSO crossing". We recall that we define: (i) the "r-LSO" (by the requirement $r(t) = r_{\rm LSO}(\nu)$), (ii) the "j-LSO" ($j(t) = j_{\rm LSO}(\nu)$), and (iii) the "ω-LSO" ($\widehat{\omega}(t) = \widehat{\omega}_{\rm LSO}(\nu)$). [In addition, one can also define an "energy-LSO", and a "naive" LSO such that $R = 6$GM.] We see from our results above that the r-LSO corresponds (in the ρ-approximation) to $\rho = 0$, while the j-LSO corresponds to $\tau = 0$, and the ω-LSO to $\rho + 0.1575\, \nu^{2/5}\, \tau = 0$. From these results and the results displayed in Fig. 7 and Eqs. (4.42) and (4.43), we have the following ordering between these LSO's: ω-LSO $<$ r-LSO $<$ j-LSO,

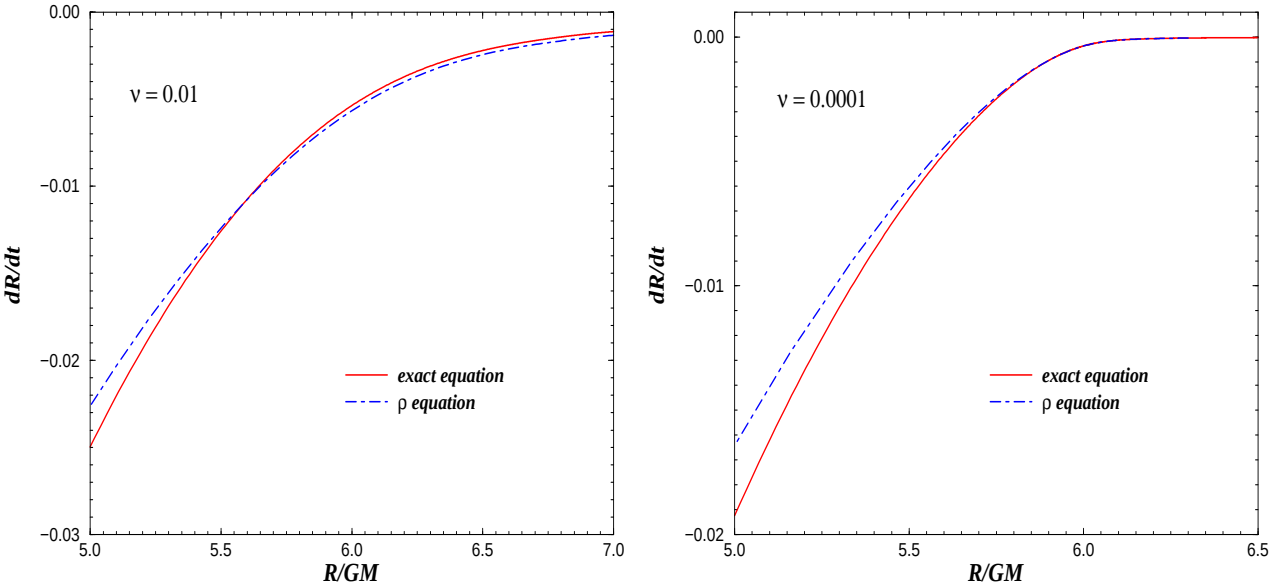

FIG. 9. *We compare the radial velocity evaluated with the exact dynamical system and with the ρ-equation in the cases $\nu = 0.01$ and $\nu = 0.0001$.*

where the order symbols refer to the location on the radial axis. We see also that when $\nu^{2/5} \ll 1$ the ω-LSO nearly coincides with the r-LSO. When discussing scaling relations it would be essentially equivalent to use any definition of LSO-crossing. For definiteness, and for consistency with the rest of this paper where we shall use it, we shall consider the ω-LSO (because it is more invariantly defined than the r-LSO). To sufficient approximation for determining the leading scaling with ν, we shall consider that the ω-LSO corresponds to $\rho \simeq 0$.

One of the most useful scaling law to consider is that concerning the radial momentum at the ω-LSO. Combining Eqs. (4.26) and (4.45) we get:

$$p_r = \frac{1}{C_r^{\rm LSO}} \frac{dr}{d\hat{t}} = \frac{1}{C_r^{\rm LSO}} \, (A_r^{\rm LSO})^{-2/5} \, (B_r^{\rm LSO})^{3/5} \, \frac{d\rho}{d\tau} \, . \tag{4.51}$$

From Eq. (4.43) the value of $d\rho/d\tau$ at the ω-LSO (i.e. $\rho \simeq 0$) is $d\rho/d\tau \simeq -0.8233$. Using also the numerical values (taken when $\nu \to 0$) of the coefficients entering Eq. (4.51), we get the predicted scaling

$$(p_r)_{\omega-{\rm LSO}} \simeq -0.0844 \, (4\nu)^{3/5} \, . \tag{4.52}$$

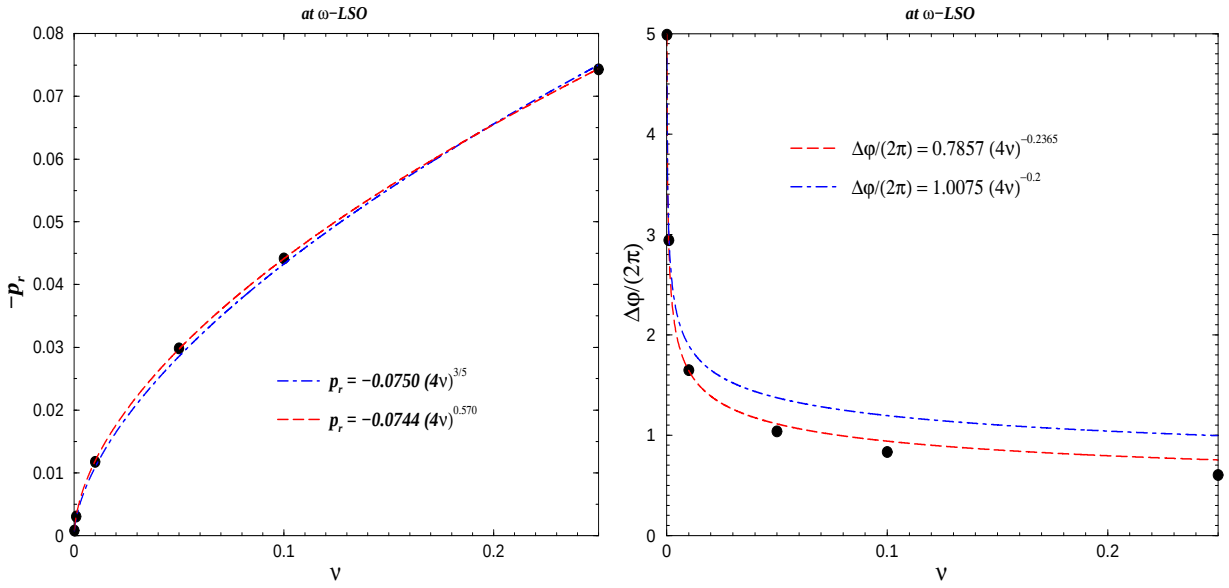

FIG. 10. *Scaling laws for the radial momentum and the post-LSO number of orbits provided by the ρ-approximation. On the left panel we show the exact numerical results for the radial momentum obtained by integrating the full evolution system down to the ω-LSO. Two fits of the type $p_r = -a\,(4\nu)^{3/5}$ and $p_r = -a\,(4\nu)^{b}$ are also indicated. On the right panel the number of orbits remaining "after LSO-crossing" is compared with the numerical results computed from the exact evolution. We have indicated both the best fit to a formula of the type $\Delta\varphi/2\pi = a\,(4\nu)^{-1/5}$, and of the type $\Delta\varphi/2\pi = a\,(4\nu)^{b}$. Note that, even if the figure covers the range of values of ν up to $1/4$, both fits have been evaluated including values only up to $\nu_{\rm max} = 0.05$.*

In the left panel of Fig. 10 we compare the analytical scaling prediction, $(p_r)_{\omega-\rm LSO} \propto (4\nu)^{3/5}$, with the numerical results obtained by integrating the full evolution system (3.41)–(3.44) down to the ω-LSO. We have also computed the best fits to the data using either a formula with one free parameter, of the type $p_r = -a\,(4\nu)^{3/5}$ or with two free parameters, $p_r = -a\,(4\nu)^{b}$. Note that the predicted scaling is a surprisingly good fit to the exact results, even for values of ν much larger than the domain of validity of the ρ-equation. In fact, it is numerically quite accurate even for $\nu = 1/4$. [In the one-parameter fit, note that the best-fit coefficient $a = 0.0750$ is 11% smaller than the calculated one, Eq. (4.52). This is because the best-fit one takes into account the values of p_r for larger values of ν than the test-mass-limit result (4.52).]

Another useful scaling law concerns the number of orbits remaining "after LSO-crossing". Let us define the number of orbits after LSO-crossing as $\Delta\varphi/2\pi$ where $\Delta\varphi$ is the difference in orbital phase between the "light-ring" $r = r_{\rm light-ring}(\nu)$ (obtained from Eq. (4.7)) and the ω-LSO, $\omega = \omega_{\rm LSO}(\nu)$. This quantity cannot be really estimated within the ρ-approximation, because this approximation assumes that $\delta r \ll 1$. However, we can formally say that, within the ρ-approximation, we wish to consider the asymptotic limit where ρ tends to $-\infty$ proportionally to $\nu^{-2/5}$ (so that δr is finite). The question is therefore: what is the asymptotic behaviour of the solution $\rho = \rho(\tau)$ of Eq. (4.38) when $\rho \to -\infty$? It seems that in this limit the "source term" $-\tau$ on the RHS of Eq. (4.38) is relatively negligible. Indeed, let us neglect it and solve the approximate equation $\frac{d^2\rho}{d\tau^2} + \frac{1}{2}\rho^2 = 0$. This equation describes the motion of a particle ($\ddot{\rho} = -\partial V(\rho)/\partial\rho$) with potential energy $V(\rho) = \rho^3/6$. This potential energy (which represents the effective radial potential near the inflection point corresponding to the LSO) is unboundedly negative when $\rho \to -\infty$. Writing the conservation of "energy", $\frac{1}{2}\dot{\rho}^2 + V(\rho) = {\rm const}$, one finds that, as $\rho \to -\infty$, the kinetic energy grows without bound and approximately satisfy $\frac{1}{2}\dot{\rho}^2 \approx -V(\rho)$ whose solution is

$$\rho = -12\,(\tau_\infty - \tau)^{-2} \tag{4.53}$$

for some constant τ_∞. We conclude that, as $\rho \to -\infty$, the variable τ tends to a finite limit τ_∞. [We find $\tau_\infty \simeq 3.9$. The corresponding curve is shown in the left panel of Fig. 7.] Therefore, from Eq. (4.53), the total time elapsed after the LSO, $\hat{t}_\infty - \hat{t}_{\rm LSO}$, scales like $\nu^{-1/5}$. Correspondingly, within the ρ-approximation, the leading approximation to the orbital phase (obtained by integrating the zeroth order term in Eq. (4.53)) reads

$$\frac{\Delta\varphi}{2\pi} = \int_{\hat{t}_{\rm LSO}}^{\hat{t}_\infty} \frac{\widehat{\omega}}{2\pi}\, d\hat{t} \simeq \frac{\widehat{\omega}_{\rm LSO}}{2\pi}\,(\hat{t}_\infty - \hat{t}_{\rm LSO}) = \frac{\widehat{\omega}_{\rm LSO}}{2\pi}\,(A_r^{\rm LSO}\,B_r^{\rm LSO})^{-1/5}\,\tau_\infty\,. \tag{4.54}$$

As $\widehat{\omega}_{\rm LSO}$ admits a finite limit as $\nu \to 0$, we expect from Eq. (4.54) the scaling law

$$\frac{\Delta\varphi}{2\pi} \propto (4\,\nu)^{-1/5}\,. \tag{4.55}$$

This prediction is compared in Fig. 10 with the numerical results obtained by integrating the full system (3.41)–(3.44). As expected from the necessity to inconsistently consider parametrically large values of $\rho \propto \nu^{-2/5}$, this prediction is less accurate than that obtained for the radial momentum at the ω-LSO. We have indicated both the best fit to a formula of

the type $\Delta\varphi/2\pi = a\,(4\nu)^{-1/5}$, and the best fit to $\Delta\varphi/2\pi = a\,(4\nu)^{b}$. Note that, both fits have been evaluated including values of ν only up to $\nu_{\rm max} = 0.05$. Indeed, as discussed above, beyond this value the fractional error in the radial velocity at the $r_{\rm LSO}$ is $\sim 10\%$.

Some comments are in order concerning these results. First, we note that although $N^{\rm after}_{\rm LSO} = \Delta\varphi/2\pi$ tends to infinity when $\nu \to 0$, it does so very slowly so that the total number of orbits after the LSO is always quite small compared to the number of orbits "just before and around the LSO". Let us define the latter number as $N^{\rm around}_{\rm LSO} \equiv f^2_{\rm orbit.}/\dot{f}_{\rm orbit.} = \frac{1}{2}\, f^2_{\rm GW}/\dot{f}_{\rm GW}$ where $f_{\rm orbit.} = \frac{1}{2}\, f_{\rm GW} = \omega/2\pi$ denotes the orbital frequency, and $\dot{f}_{\rm orbit.}$ the time derivative of the orbital frequency caused by GW damping. In the adiabatic approximation, combined with a Newtonian approximation for both the orbital energy and the GW flux, this number reads (see, e.g., [5])

$$N^{\rm around}_{\rm LSO} \simeq \frac{2.924}{4\nu}\,. \tag{4.56}$$

The ratio $N^{\rm after}_{\rm LSO}/N^{\rm around}_{\rm LSO} \simeq 0.3446\,(4\nu)^{4/5}$ (derived using the result of the fit, i.e. $N^{\rm after}_{\rm LSO} = 1.0075\,(4\nu)^{-1/5}$) is therefore *parametrically* small as $\nu \to 0$. This suggests that, when $4\nu \ll 1$, the existence of even a formally parametrically large ($\propto \nu^{-1/5}$) absolute number of cycles left after the LSO will have only a fractionally negligible effect on the extraction of a GW signal from the noise by means of relativistic filters built on the adiabatic approximation, and terminated at the LSO [6], [5]. On the other hand, when $4\nu \sim 1$ the ratio $N^{\rm after}_{\rm LSO}/N^{\rm around}_{\rm LSO}$ is not very small. In particular, when $\nu = 1/4$ the number of orbits after the ω-LSO is equal to $N^{\rm after}_{\rm LSO}(\nu = 1/4) = 0.6024$ (computed from the exact evolution), while $N^{\rm around}_{\rm LSO}(\nu = 1/4) = 2.924$. The ratio between the two is $N^{\rm after}_{\rm LSO}/N^{\rm around}_{\rm LSO} = 0.2060$. As recently emphasized in Ref. [5], the fact that $N^{\rm around}_{\rm LSO}$ is not large means that the filtering of such a signal out of the noise is a delicate matter which sensitively depends on the modeling of the phase evolution near the LSO, and on the modeling of what happens to the signal after LSO crossing. In Ref. [5] it was assumed that the signal is abruptly terminated at the LSO. In a later section we shall use the tools introduced here to go beyond such an approximation and study the part of the waveform which is emitted after LSO crossing.

V. INITIAL DATA FOR NUMERICAL RELATIVITY

One of the main aims of this paper is to use the improved approach to the transition from the inspiral to the plunge introduced above to compute initial dynamical data (i.e. initial positions and momenta) for binary black holes that have just started their plunge motion. Ideally, we wish to give dynamical data for two black holes $(\boldsymbol{q}_1, \boldsymbol{q}_2, \boldsymbol{p}_1, \boldsymbol{p}_2)$ such that the coordinate distance $|\boldsymbol{q}_1 - \boldsymbol{q}_2|$ is: (i) large enough that one can trust the re-summed non-perturbative technique allowing one to compute these data; (ii) large enough to allow one to hope to complete the present work by constructing the initial gravitational data $(g_{ij}(x), K_{ij}(x))$ determined (in principle) by $(\boldsymbol{q}_a, \boldsymbol{p}_a)$; and, finally (iii) small enough to leave only less than one orbit (at least when $\nu \sim 1/4$) to evolve by means of a full 3D numerical relativity code. We think that the point (i) is satisfied if we use the Padé-type [6] plus effective-one-body [7] methods we have combined above, *and* if we stop the evolution of quasi-circular orbits anywhere around the LSO. We shall leave the point (ii), i.e. the important task of completing the present work by constructing gravitational data to future work. However, in preparation for this task we shall show how one can compute the dynamical data $(\boldsymbol{q}_a, \boldsymbol{p}_a)$ in the convenient ADM coordinates. Indeed, the coordinate conditions introduced by Arnowitt, Deser and Misner [27] have the double advantage: (a) to be linked to the $3+1$ formulation which is used in numerical relativity, and (b) to be linked to explicit, high-order post-Newtonian calculations [17]. Concerning the point (iii), the work above shows that if we stop the inspiral + plunge evolution at the (invariantly defined) ω-LSO (i.e. when $d\varphi/dt = \omega_{\rm LSO}(\nu)$) there indeed remains (when $4\nu \sim 1$) less than one orbit to go before reaching the light-ring (see next section for a discussion of the importance of the light-ring). Note that there is nothing sacred about giving data precisely at the ω-LSO. Because of the points (i) and (ii) above we wish to stay "as high as possible". Because of point (iii) we must, however, be just after LSO crossing. As was already discussed, there are several possible definitions of "LSO crossing". The ω-LSO is the innermost LSO (see below) and is therefore a convenient choice (however, there would be nothing wrong in giving data at a slightly different place; in fact we recommend to do it to check the robustness of the numerical spacetimes evolved from our data).

As just recalled we wish to (numerically) compute complete dynamical data at the ω-LSO, and in ADM coordinates. The evolution system (3.41)–(3.44) given above allows one to

compute dynamical data $(r, \varphi, p_r, p_\varphi)$ for the relative motion described in (reduced) *effective* coordinates (i.e. the coordinates used in the effective-one-body description). In Ref. [7] we have shown how to map the ADM positions and momenta $(q^{\rm ADM}, p^{\rm ADM})$ onto the effective positions and momenta (q, p) by means of a generating function $G(q^{\rm ADM}, p)$. Let us first recall, in order to avoid any confusion, the trivial transformations linking Cartesian-like to polar-like coordinates, as well as those linking the original to the scaled coordinates. We recall that we work in the center of mass frame and that we consider planar motion in the equatorial plane $\theta = \pi/2$:

$$Q^i = q_1^i - q_2^i \,, \qquad P_i = p_{1i} = -p_{2i} \,, \tag{5.1}$$

$$P_R = n^i \, P_i \,, \qquad P_\varphi = Q^x \, P_y - Q^y \, P_x \,, \tag{5.2}$$

$$q^i = \frac{Q^i}{GM} \,, \qquad p_i = \frac{P_i}{\mu} \,, \tag{5.3}$$

$$p_r = \frac{P_R}{\mu} = n^i \, p_i \,, \qquad p_\varphi = \frac{P_\varphi}{\mu \, GM} = q^x \, p_y - q^y \, p_x \,. \tag{5.4}$$

Here $n^i = Q^i/R = q^i/r$ is the radial unit vector ($R = |\boldsymbol{Q}|$, $r = |\boldsymbol{q}|$). We have also $Q^x = R\cos\varphi$, $Q^y = R\sin\varphi$, $q^x = r\cos\varphi$, $q^y = r\sin\varphi$. The relations above hold both in effective coordinates (denoted by (q^i, p_i) without extra labels) and in ADM coordinates $(q^i_{\rm ADM}, p_i^{\rm ADM})$. The link between (q^i, p_i) and $(q^i_{\rm ADM}, p_i^{\rm ADM})$ is defined by a generating function $G(q^i_{\rm ADM}, p_i)$ and reads

$$q^i = q^i_{\rm ADM} + \frac{\partial \, G(q^{\rm ADM}, p)}{\partial \, p_i} \,, \tag{5.5}$$

$$p_i^{\rm ADM} = p_i + \frac{\partial \, G(q^{\rm ADM}, p)}{\partial \, q^i_{\rm ADM}} \,. \tag{5.6}$$

The generating function G has been derived up to 2PN order in [7] (see Ref. [15] for the determination of G at the 3PN level)

$$G(q^{\rm ADM}, p) = \frac{1}{c^2} \, G_{\rm 1PN}(q^{\rm ADM}, p) + \frac{1}{c^4} \, G_{\rm 2PN}(q^{\rm ADM}, p) \,. \tag{5.7}$$

The partial derivatives needed in Eqs. (5.5), (5.6) read

$$\frac{\partial G_{\rm 1PN}(q,p)}{\partial q^i} = p_i \left[-\frac{\nu}{2}\,\boldsymbol{p}^2 + \left(1+\frac{\nu}{2}\right)\,\frac{1}{q} \right] - q_i\,(\boldsymbol{q}\cdot\boldsymbol{p})\,\left(1+\frac{\nu}{2}\right)\,\frac{1}{q^3}\,, \tag{5.8}$$

$$\frac{\partial G_{\rm 1PN}(q,p)}{\partial p_i} = q^i \left[-\frac{\nu}{2}\,\boldsymbol{p}^2 + \left(1+\frac{\nu}{2}\right)\,\frac{1}{q} \right] - p^i\,(\boldsymbol{q}\cdot\boldsymbol{p})\,\nu\,, \tag{5.9}$$

$$\begin{aligned}\frac{\partial G_{\rm 2PN}(q,p)}{\partial q^i} = p_i & \left[\frac{1}{8}\,\nu\,(1+3\,\nu)\,\boldsymbol{p}^4 + \frac{\nu}{8}\,(2-5\,\nu)\,\frac{\boldsymbol{p}^2}{q} + \frac{3}{8}\,\nu\,(8+3\,\nu)\,\frac{(\boldsymbol{q}\cdot\boldsymbol{p})^2}{q^3} \right. \\ & \left. + \frac{1}{4}\,(1-7\,\nu+\nu^2)\,\frac{1}{q^2} \right] + q_i\,(\boldsymbol{q}\cdot\boldsymbol{p}) \left[-\frac{3}{8}\,\nu\,(8+3\,\nu)\,\frac{(\boldsymbol{q}\cdot\boldsymbol{p})^2}{q^5} \right. \\ & \left. - \frac{\nu}{8}\,(2-5\,\nu)\,\frac{\boldsymbol{p}^2}{q^3} - \frac{1}{2}\,(1-7\,\nu+\nu^2)\,\frac{1}{q^4} \right]\,, \end{aligned} \tag{5.10}$$

$$\begin{aligned}\frac{\partial G_{\rm 2PN}(q,p)}{\partial p_i} = q^i & \left[\frac{1}{8}\,\nu\,(1+3\,\nu)\,\boldsymbol{p}^4 + \frac{\nu}{8}\,(2-5\,\nu)\,\frac{\boldsymbol{p}^2}{q} + \frac{3}{8}\,\nu\,(8+3\,\nu)\,\frac{(\boldsymbol{q}\cdot\boldsymbol{p})^2}{q^3} \right. \\ & \left. + \frac{1}{4}\,(1-7\,\nu+\nu^2)\,\frac{1}{q^2} \right] + p^i\,(\boldsymbol{q}\cdot\boldsymbol{p}) \left[\frac{\nu}{2}\,(1+3\,\nu)\,\boldsymbol{p}^2 + \frac{\nu}{4}\,(2-5\,\nu)\,\frac{1}{q} \right]\,. \end{aligned} \tag{5.11}$$

Given q^i and p_i, we use first Eq. (5.5), and the values of the partial derivatives (5.8)–(5.11), to solve numerically for $q^i_{\rm ADM}$. Then we use Eq. (5.6) to compute $p_i^{\rm ADM}$:

The initial data we start with are the results of the numerical integration of the system (3.41)–(3.44), i.e. the values of r, φ, p_r and p_φ at some time in the evolution (which we choose to be the time when $\omega(t) = \omega_{\rm LSO}(\nu)$). Actually, the value of φ is without significance and we renormalize it to the convenient value $\varphi_{\rm new} = 0$ so that we work with Cartesian-like data of the simple form (remember that we work in the $x-y$ plane, $q^z = 0 = p_z$, and that we simplify the writing by denoting $q_i \equiv q^i$ when working in Cartesian-like coordinates)

$$q_x = r\,, \qquad q_y = 0\,, \qquad p_x = p_r\,, \qquad p_y = \frac{p_\varphi}{r}\,. \tag{5.12}$$

When solving, as indicated above, Eqs. (5.5), (5.6) to derive $q_x^{\rm ADM}$, $q_y^{\rm ADM}$ and $p_x^{\rm ADM}$, $p_y^{\rm ADM}$, we get these quantities in a not optimally oriented coordinate system (i.e. though we started with $q_y = 0$, we end up with $q_y^{\rm ADM} \neq 0$ because there is a rotation between the two coordinate systems). As the global orientation is of no physical significance, it is convenient to turn the ADM coordinate system by an angle α so that $\varphi_{\rm new}^{\rm ADM} = \varphi_{\rm old}^{\rm ADM} - \alpha = 0$. In other words, after this rotation one has, as in Eq. (5.12) above,

$$q_x^{\rm ADM\,new} = r^{\rm ADM}\,, \quad q_y^{\rm ADM\,new} = 0\,, \quad p_x^{\rm ADM\,new} = p_r^{\rm ADM}\,, \quad p_y^{\rm ADM\,new} = \frac{p_\varphi^{\rm ADM}}{r^{\rm ADM}}\,. \tag{5.13}$$

The angle of rotation α is determined by

ν	$r^{\rm ADM}$	$p_r^{\rm ADM}$	$p_t^{\rm ADM}$	$p_\varphi^{\rm ADM}$	α
0.25	4.717	-0.07570	0.7021	3.312	-0.006256
0.1	4.853	-0.04425	0.6997	3.396	-0.001524
0.01	4.938	-0.01163	0.6996	3.455	$-4.088 \cdot 10^{-5}$
0.001	4.948	-0.002992	0.6998	3.463	$-1.054 \cdot 10^{-6}$
0.0001	4.949	-0.0007592	0.6999	3.464	$-2.675 \cdot 10^{-8}$

TABLE I. *Initial data in ADM coordinates at ω-LSO for five representative values of ν.*

$$\tan\alpha = \frac{q_y^{\rm ADM\,old}}{q_x^{\rm ADM\,old}}\,, \tag{5.14}$$

while the more invariant quantities $r^{\rm ADM}$ and $p_r^{\rm ADM}$ are given by

$$r^{\rm ADM} \equiv \sqrt{(q_{x\,\rm old}^{\rm ADM})^2 + (q_{y\,\rm old}^{\rm ADM})^2}\,, \quad p_r^{\rm ADM} \equiv \frac{1}{r^{\rm ADM}}\left(q_{x\,\rm old}^{\rm ADM}\, p_{x\,\rm old}^{\rm ADM} + q_{y\,\rm old}^{\rm ADM}\, p_{y\,\rm old}^{\rm ADM}\right). \tag{5.15}$$

Note that (because of the rotational invariance of G) all the angular momenta coincide:

$$p_\varphi = p_\varphi^{\rm ADM} = q_x\, p_y - q_y\, p_x = q_{x\,\rm old}^{\rm ADM}\, p_{y\,\rm old}^{\rm ADM} - q_{y\,\rm old}^{\rm ADM}\, p_{x\,\rm old}^{\rm ADM} = q_{x\,\rm new}^{\rm ADM}\, p_{y\,\rm new}^{\rm ADM} - q_{y\,\rm new}^{\rm ADM}\, p_{x\,\rm new}^{\rm ADM}\,. \tag{5.16}$$

This relation is a useful check on the numerical precision of the solution of Eqs. (5.5), (5.6).

In Tab. I we give initial data in ADM coordinates at the ω-LSO for five values of the parameter ν. We give the more invariant quantities corresponding to the "new" ADM coordinate system Eq. (5.13). The quantity $p_t^{\rm ADM}$ denotes the "transverse" momentum, i.e. simply $p_t^{\rm ADM} \equiv p_\varphi^{\rm ADM}/r^{\rm ADM} \equiv p_{y\,\rm new}^{\rm ADM}$. For completeness, we give also the value of the angle α, Eq. (5.14).

So far all the results we have discussed considered the evolution system (3.41)–(3.44) as the "exact" description of the transition through the LSO. However, as discussed in Sec. III this system is more like a convenient fiducial system within a class of systems obtained by shifting (by $\mathcal{O}(v^5/c^5)$ terms) the coordinate system. To test the robustness of our predictions for physical quantities at the LSO we shall now compare the results of the fiducial system (3.41)–(3.44) with the results obtained by the more general system (3.4)–(3.7), with a radial force $\mathcal{F}_R$ given (in terms of $\mathcal{F}_\varphi$) by Eq. (3.20). For simplicity, we consider only the (most

crucial) equal-mass case, $\nu = 1/4$. We find that our fiducial system (with $\mathcal{F}_R = 0$) yields the following numerical values at the ω-LSO (when starting with an orbital phase $\varphi = 0$ at $r = 15$)

$$r = 5.639\,, \qquad p_r = -0.07432\,, \qquad \dot{r} = -0.03563\,, \tag{5.17}$$

$$\varphi = 82.72\,, \qquad j = 3.312\,, \qquad \frac{\mathcal{E}^{\rm NR}_{\rm real}}{M} = -0.01640\,. \tag{5.18}$$

On the other hand, the system including the non-zero radial force (3.20) yields at the ω-LSO (still starting with an orbital phase $\varphi = 0$ at $r = 15$)

$$r = 5.638\,, \qquad p_r = -0.07388\,, \qquad \dot{r} = -0.03542\,, \tag{5.19}$$

$$\varphi = 82.77\,, \qquad j = 3.311\,, \qquad \frac{\mathcal{E}^{\rm NR}_{\rm real}}{M} = -0.01643\,. \tag{5.20}$$

As we see the differences in the numerical results are quite small. For instance, the fractional change in the (crucial) radial momentum is less than 6×10^{-3}. We note also that the dephasing at the LSO is only 0.05 radians. This analysis indicates that the results based on our fiducial system are quite robust, mainly because our basic assumption of "quasi-circularity" ($\dot{R} \ll R\,\dot{\varphi}$) is well satisfied during the transition to the plunge.

VI. GRAVITATIONAL WAVE-FORMS FROM INSPIRAL TO RING-DOWN

In this section, we provide, for data analysis purposes, an estimate of the complete waveform emitted by the coalescence of two black holes (with negligible spins). This estimate will be less accurate than our results above because we shall extend the integration of our basic system (3.41)–(3.44) beyond its range of validity. We think, however, that even a rough estimate of the complete waveform (exhibiting the way the inspiral waveform smoothly transforms itself in a "plunge waveform" and then into a "merger plus ring-down" waveform) is a very valuable information for designing and testing effectual gravitational wave templates. [See, in particular, the recent work [5] which emphasizes the importance of the details of the transition to the plunge for the construction of faithful GW templates for massive binaries.]

Our (rough) assumptions in this section will be the following: (i) we use the basic evolution system (3.41)–(3.44) to describe the dynamics of the binary system from deep into the inspiral phase (say $r \simeq 15$) down to the "light-ring" $r = r_{\rm light-ring}(\nu) \simeq 3$; (ii) we estimate

the waveform emitted during the inspiral and the plunge by means of the usual "restricted waveform" approximation

$$\hat{t} \leq \hat{t}_{\rm end}: \quad h_{\rm inspiral}(\hat{t}) = \mathcal{C}\, v_\omega^2(\hat{t}) \cos(\phi_{\rm GW}(\hat{t}))\,, \quad v_\omega \equiv \left(\frac{d\varphi}{d\hat{t}}\right)^{\frac{1}{3}}, \quad \phi_{\rm GW} \equiv 2\varphi\,, \tag{6.1}$$

and (iii) we estimate the waveform emitted during the coalescence and ring-down by matching, at a time $\hat{t} = \hat{t}_{\rm end}$ where the light-ring is crossed, the inspiral + plunge waveform (6.1) to the least-damped quasi-normal mode of a Kerr black hole with mass and spin equal to the total energy and angular momentum of the plunging binary (at $\hat{t} = \hat{t}_{\rm end}$):

$$\hat{t} \geq \hat{t}_{\rm end}: \quad h_{\rm merger}(\hat{t}) = \mathcal{A}\, e^{-(\hat{t}-\hat{t}_{\rm end})/\tau} \cos(\omega_{\rm qnm}\,(\hat{t}-\hat{t}_{\rm end}) + \mathcal{B})\,. \tag{6.2}$$

For convenience, we shall normalize the waveform by taking $\mathcal{C} = 1$ in Eq. (6.1). The amplitude $\mathcal{A}$ and the phase $\mathcal{B}$ of the merger waveform (6.2) are then determined by requiring the continuity of $h(\hat{t})$ and $dh/d\hat{t}$ at the matching point $\hat{t} = \hat{t}_{\rm end}$.

Before giving technical details let us comment on our assumptions (i)–(iii). First, we recall that Fig. 1 had shown that the quasi-circularity condition $p_r^2/B(r) \ll p_\varphi^2/r^2$ (which is the basic condition determining the validity of our evolution system) was satisfied with good accuracy during the inspiral and the beginning of the plunge, and was still satisfied, though with less accuracy ($p_r^2/B \lesssim 0.3\, p_\varphi^2/r^2$ in the worst case $\nu = 1/4$) down to the light-ring $r \simeq 3$. In other words, our work is showing that the so called "plunge" following the inspiral phase is better thought of as being still a quasi-circular inspiral motion, even down to the light-ring. We therefore expect that the usual restricted waveform (6.1) (valid for circular motion) will be an acceptable description of the GW emission during the plunge. Note that we consider that the description of the amplitude of the gravitational wave in terms of $v_\omega^2 \equiv \dot{\varphi}^{2/3}$, being simpler and more invariant, has a better chance of being correct than a description in terms of some other Newtonian-like approximation to the "squared velocity" such as $(r\,\dot{\varphi})^2$ or $1/r$. Some evidence for this faith is given by the fact that the GW flux is surprisingly well approximated (within 10% down to the LSO) by the usual "quadrupole formula" *if* the velocity used to define the quadrupole formula is the invariant $v_\omega = \dot{\varphi}^{1/3}$ (see, e.g., Fig. 3 of [6]).

Concerning the choice of the light-ring for shifting the description between a (quasi-circular) binary motion and a deformed Kerr black hole, our motivation is twofold. First, in the test-mass limit, $\nu \ll 1$, it has been realized long ago, in the first work [28] which

found the existence of a merger signal of the type (6.2) following a plunge event, that the basic physical reason underlying the presence of a "universal" merger signal was that when a test particle falls below $R \simeq 3GM$, the GW it generates is strongly filtered by the potential barrier, centered around $R \simeq 3GM$, describing the radial propagation of gravitational waves. It was then realized [29] that the peaking of the potential barrier around $R \simeq 3GM$ is itself linked to the presence of an unstable "light storage ring" (i.e. an unstable circular orbit for massless particles) precisely at $R = R_{\rm light-right} = 3GM$. A second argument (applying now in the equal-mass case, $\nu = 1/4$) indicating that $r_{\rm light-right}(1/4) \simeq 2.84563$ is an acceptable divide between the two-body and the perturbed-black-hole descriptions comes from the works on the, so called, "close limit approximation" [30]. Indeed, recent work (see the review [31]) suggests a matching between the two-body and the perturbed-black-hole descriptions when the distance modulus $\mu_0 \simeq 2$. Using the formulas of Ref. [32] one finds that $\mu_0 \simeq 2$ corresponds to a coordinate distance in isotropic coordinates of $r^{\rm iso} \simeq \sqrt{2} x GM$. This corresponds to a Schwarzschild-like radial distance $R \simeq r\,(1 + GM/2r)^2 \simeq 2.59GM$ which is not very far from $R_{\rm light-ring}(1/4) \simeq 2.84GM$.

In keeping with our prescription of setting the divide between a binary-black-hole description and a perturbed-single-black-hole one, at the time $\hat{t}_{\rm end}$, when $r \simeq r_{\rm light-ring}(\nu)$, it is natural to assume that the final hole formed by the merger is a Kerr hole with mass $M_{\rm BH}$ and angular momentum $\mathcal{J}_{\rm BH}$ given by:

$$\frac{M_{\rm BH}}{\mu} \equiv \widehat{H}_{\rm end} = \frac{1}{\nu}\sqrt{1 + 2\nu\,(\widehat{H}^{\rm end}_{\rm eff} - 1)}\,, \qquad j_{\rm end} \equiv \frac{\mathcal{J}_{\rm BH}}{\mu\, G\, M}\,, \tag{6.3}$$

while the dimensionless rotation parameter $\widehat{a}$ is:

$$\widehat{a}_{\rm BH} \equiv \frac{\mathcal{J}_{\rm BH}}{G\, M^2_{\rm BH}} = \frac{\nu\, j_{\rm end}}{1 + 2\nu\,(\widehat{H}^{\rm end}_{\rm eff} - 1)}\,. \tag{6.4}$$

As the system reaches the stationary Kerr state, the non-linear dynamics of the merger becomes more and more describable in terms of oscillations of the black hole quasi-normal modes [33]. During this phase, often called the ring-down phase, the gravitational signal will be a superposition of exponentially damped sinusoids. The gravitational waveform will be dominated by the $l = 2, m = 2$ quasi-normal mode, which is the most slowly damped mode.

As a rough approximation we assume that the full merger + ring-down signal (starting when the light-ring is reached) can be represented in terms of this least damped quasi-normal mode. If ω_{qnm} denotes the circular frequency of this mode, and τ its damping time, this leads

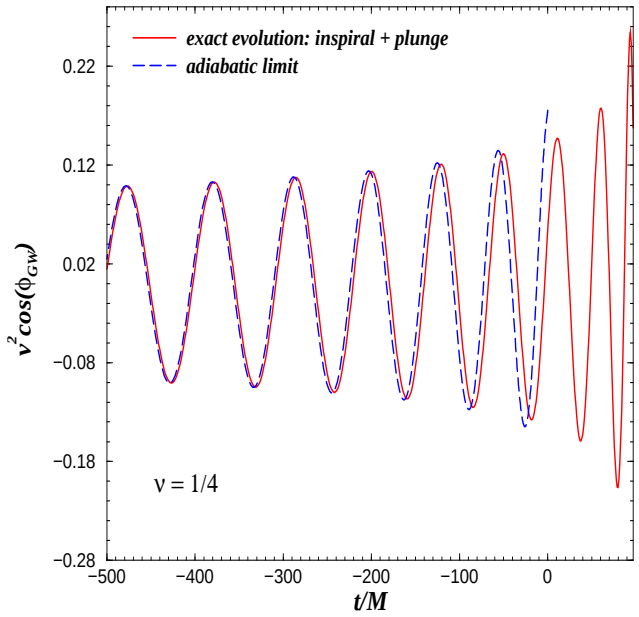

FIG. 11. *We compare the inspiral + plunge waveform, terminated at the light-ring, to the adiabatic waveform, terminated at the adiabatic LSO.*

to the simple description (6.2). The quantities (ω_{qnm}, τ) are functions of $(M_{\rm BH}, \widehat{a}_{\rm BH})$ which have been investigated numerically [33], [34]. Using analytic fits the following expressions for the frequency and the decay time of the quasi-normal modes were obtained [35]

$$M_{\rm BH}\,\omega_{\rm qnm} = \left[1 - 0.63\,(1-\widehat{a})^{3/10}\right]\; f_f(\widehat{a})\,, \tag{6.5}$$

$$\tau\,\omega_{\rm qnm} = 4\,[1-\widehat{a}]^{-9/20}\; f_Q(\widehat{a})\,, \tag{6.6}$$

where $f_f(\widehat{a})$ and $f_Q(\widehat{a})$ are correction factors provided by Tab. 2 of [35]. Note that $f_f = 0.9587$ and $f_Q = 1.0501$ for $\widehat{a} = 10^{-4}$.

We have numerically studied only the equal-mass case $\nu = 1/4$. We have chosen the matching point $\hat{t}_{\rm end}$ such that $r\,(\hat{t}_{\rm end}) = r_{\rm light-ring}(1/4) = 2.84563$. With this value of $\hat{t}_{\rm end}$ we obtain the following values for the characteristics of the formed black hole:

$$\widehat{a}_{\rm BH} = 0.7952\,, \qquad E_{\rm BH} = 0.9761\,M\,, \tag{6.7}$$

$$M\,\omega_{\rm qnm} = 0.5976\,, \qquad M/\tau = 0.07795\,. \tag{6.8}$$

Note the numerical value of the quasi-normal mode frequency

$$f_{\rm qnm} \simeq \frac{\omega_{\rm qnm}}{2\pi} = 1885\,\left(\frac{10\,M_\odot}{M_{\rm BH}}\right)\,{\rm Hz}\,. \tag{6.9}$$

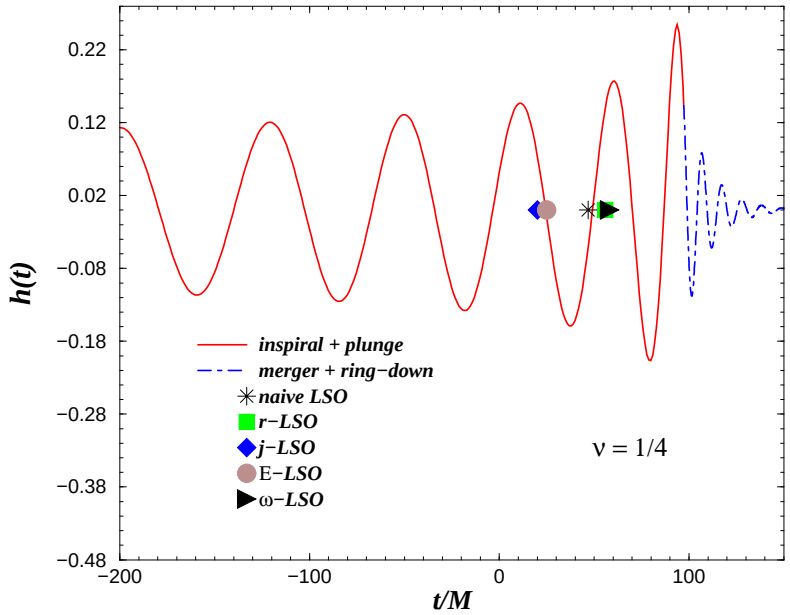

FIG. 12. *Plot of the complete waveform: inspiral and plunge followed by merger and ring-down. The locations of several possible definitions of LSO crossing are also indicated.*

Our results for the waveform are shown in Figs. 11 and 12. In Fig. 11 we compare the inspiral + plunge waveform (6.1) (terminated at the light-ring) to the usually considered adiabatic waveform (terminated at the "adiabatic LSO"). As already discussed in Section IV, by "adiabatic waveform" we mean a restricted waveform (6.1) (with $\mathcal{C} = 1$) in which $\varphi(\hat{t}) = \varphi_{\rm adiab.}(\hat{t})$ is defined by integrating the two equations (4.11) and (4.12). This Figure shows that there is a significant dephasing of the adiabatic waveform with respect to the (more) exact one already before the LSO. Moreover, the real inspiral signal continues to increase and oscillate for $\simeq 2.35$ cycles after the adiabatic LSO.

In Fig. 12 we plot our estimate of the complete waveform: inspiral and plunge (solid line) followed by merger and ring-down (dashed line). We also indicated the locations of several possible definitions of LSO crossing (see Section IV above). In addition to the definitions mentioned above we also included a "naive LSO" (defined simply by $r^{\rm naive}_{\rm LSO} \equiv 6$ as in the Schwarzschild geometry) and an energy-LSO (such that $\mathcal{E}_{\rm real}(t) = \mathcal{E}^{\rm LSO}_{\rm real}(\nu)$).

The corresponding numerical values of the reduced radial coordinate r are:

$$r_{\rm j-LS0} = 6.631\,, \qquad r^{\rm naive}_{\rm LSO} = 6.000\,, \qquad r_{\mathcal{E}-\rm LS0} = 6.534\,, \tag{6.10}$$

$$r_{\rm r-LS0} = 5.718\,, \qquad r_{\omega-\rm LS0} = 5.639\,. \tag{6.11}$$

As mentioned above, the fact that the various definitions of the LSO differ significantly is

due to the fact that when $\nu = 1/4$ the GW damping effects are rather large and blur the transition to the plunge. Note that the number of GW cycles left after the (exact) ω-LSO (and until the light-ring) is $N^{\rm after}_{\rm GW} = 2N^{\rm after}_{\rm orbit} = 1.2048$ (for $\nu = 1/4$). As said above, this is smaller than the (physically less relevant) number of cycles left after the adiabatic LSO (where $\omega \simeq 0.80\,\omega_{\rm LSO}$), which is $\simeq 2.35$.

Even if our estimate of the waveform is admittedly rough, we think that it can play an important role for defining better filters for the search of signals in LIGO and VIRGO. In particular, two features of this waveform are striking: (i) the 'plunge' part of the waveform looks like a continuation of the inspiral part (this is because the orbital motion remains in fact quasi-circular), and (ii) the adiabatic waveform gets significantly out of phase with the exact waveform before crossing the LSO. We shall come back in future work to the consequences of these results for data analysis, and see how they can be used to improve upon the state-of-the-art filters constructed in Ref. [6], [5].

VII. DISCUSSION

In this paper we have extended a methodology introduced in previous papers [6], [7], and applied it to the study of the transition from inspiral to plunge in coalescing binary black holes with comparable masses, moving on quasi-circular orbits. Our philosophy is that it is possible to use suitably re-summed versions of post-Newtonian results to write an explicit (analytical) system of ordinary differential equations describing the transition to the plunge. Our explicit proposal is the evolution system (3.41)–(3.44) obtained by combining the results of [6] for the re-summation of the gravitational wave damping, and the results of [7] for the re-summation of the conservative part of the dynamics of comparable-mass binaries. The basic reason why we think the simple evolution system (3.41)–(3.44) can accurately describe the transition to the plunge is that we have consistently checked that most of the "plunge" motion (at least down to $R \simeq 3GM$) is in fact very much like a quasi-circular inspiral motion (with $\dot{R}^2 \ll (R\,\dot{\varphi})^2$).

In general one needs to numerically integrate the basic evolution system (3.41)–(3.44) to get physical results of direct interest. However, we have shown that one can understand the various physical elements entering this system by comparing it to several simple approximations: the adiabatic approximation, the $\dot{r}$-linearized one, and the universal ρ-approximation

(valid when $\nu \lesssim 0.05$). In particular, the latter approximation allowed us to derive some scaling laws: one scaling law (which is very well satisfied, even up to the maximum value $\nu = 1/4$) states that the radial momentum at the Last Stable Orbit (LSO) scales like $\nu^{3/5}$, while another scaling law (accurately satisfied only for $\nu \ll 1$) states that the number of cycles left after the LSO scales like $\nu^{-1/5}$.

The two most important consequences of the present approach are: (i) a way to compute initial dynamical data $(\boldsymbol{q}_1, \boldsymbol{q}_2, \boldsymbol{p}_1, \boldsymbol{p}_2)$ for a comparable-mass binary black hole system, represented in ADM coordinates, such that only a fraction of an orbit needs to be further evolved by numerical relativity techniques, and (ii) an estimate of the complete waveform emitted by a binary black hole coalescence, smoothly combining an inspiral signal, a plunge signal, a merger signal and a ring-down.

However, much work remains to be done to firm up and complete our approach. We checked the robustness of our approach by considering an as-well-justified, slightly different evolution system. But stronger checks are called for. In particular it would be quite important to extend the present work (which used as input the 2.5PN-accurate damping and 2PN-accurate dynamics) to higher PN levels, when they become fully available. We note in this respect the recent work [16] which extended the effective-one-body approach to the 3PN level. [Note in passing that quasi-static tidal interactions between black holes enter only at the 5PN level [12].] It is quite important to complete our determination of initial *dynamical* data $(\boldsymbol{q}_a, \boldsymbol{p}_a)$ by explicitly constructing the initial *gravitational* data $(g_{ij}(x), K_{ij}(x))$ corresponding to $(\boldsymbol{q}_a, \boldsymbol{p}_a)$ (and containing no free incoming radiation). When this becomes available it will be possible to further check our method (by numerically evolving spacetimes starting at various stages of the plunge) and to provide more accurate estimates of the merger waveform. Though our "light-ring-matching" approach to estimating the complete waveform is admittedly rough, we think it can play a useful role for data analysis: it can be used to test the accuracy of present templates (based on the adiabatic approximation) and allow one to construct more accurate, or at least, more robust, templates. We will come back to this issue in future work. Finally, let us note that it would be, in principle, important to be able to extend our approach to black holes having significant intrinsic spins. We, however, anticipate that this is a highly non-trivial task.

ACKNOWLEDGMENTS

A.B.'s research was supported at Caltech by the Richard C. Tolman Fellowship and by NSF Grant AST-9731698 and NASA Grant NAG5-6840.

All the numerical results in the present paper were produced using Mathematica.

REFERENCES

[1] V.M. Lipunov, K.A. Postnov and M.E. Prokhorov, New Astronomy **2**, 43 (1997).

[2] E.E. Flanagan and S.A. Hughes, Phys. Rev. **D57**, 4535 (1998).

[3] P.R. Brady, J.D.E. Creighton and K.S. Thorne, Phys. Rev. **D58**, 061501 (1998).

[4] K.A. Postnov and M.E. Prokhorov, in Rencontres de Moriond, January 1999, edited by J. Tran Thanh Van et al. (Editions Frontières, Gig-sur-Yvette, 1999); [astro-ph/9903193].

[5] T. Damour, B.R. Iyer and B.S. Sathyaprakash, *Frequency-domain P-approximant filters for time-truncated gravitational waves from inspiraling compact binaries*, in preparation.

[6] T. Damour, B.R. Iyer and B.S. Sathyaprakash, Phys. Rev. **D57**, 885 (1998).

[7] A. Buonanno and T. Damour, Phys. Rev. **D59**, 084006 (1999).

[8] C.W. Lincoln and C.M. Will, Phys. Rev. **D42**, 1123 (1990).

[9] L.E. Kidder, C.M. Will and A.G. Wiseman, Class. Quantum Grav. **9**, L127 (1992); Phys. Rev. **D47**, 3281 (1993).

[10] T. Damour and N. Deruelle, Phys. Lett. **A87**, 81 (1981).

[11] T. Damour, C.R. Acad. Sci. Sér. II, **294**, 1355 (1982).

[12] T. Damour, in *Gravitational Radiation*, ed. N. Deruelle and T. Piran (North-Holland, Amsterdam, 1983), pp. 59-144.

[13] N. Wex and G. Schäfer, Class. Quantum Grav. **10**, 2729 (1993).

[14] G. Schäfer and N. Wex, in *XIIIth Moriond Workshop: Perspectives in neutrinos, atomic physics and gravitation*, (ed. by J. Trân Thanh Vân, T. Damour, E. Hinds and J. Wilkerson, Editions Frontières, Gif-sur-Yvette, 1993), pp. 513.

[15] T. Damour, P. Jaranowski and G. Schäfer, *Dynamical invariants for general relativistic two-body systems at the third post-Newtonian approximation*; [gr-qc/9912092].

[16] T. Damour, P. Jaranowski and G. Schäfer, in preparation.

[17] P. Jaranowski and G. Schäfer, Phys. Rev. **D57**, 5948 (1998); ibid. **D57**, 7274 (1998).

[18] A. Ori and K.S. Thorne, *The transition from inspiral to plunge for a compact body in a circular equatorial orbit around a massive, spinning black hole*, in preparation.

[19] G. Schäfer, Ann. Phys. **161**, 81 (1985).

[20] G. Schäfer, Gen. Rel. Grav. **18**, 255 (1986).

[21] G. Schäfer, in *Symposia Gaussiana, Proceedings of the* 2^{nd} *Gauss Symposium, Conference A: Mathematics and Theoretical Physics* (ed. by M. Behara, R. Fritsch and R. Lintz, Walter de Gruyter, Berlin, 1995), pp. 667.

[22] B.R. Iyer and C.M. Will, Phys. Rev. Lett. **70**, 113 (1993); Phys. Rev. **D52**, 6882 (1995).

[23] L. Blanchet, T. Damour, B.R. Iyer, C.M. Will and A.G. Wiseman, Phys. Rev. Lett. **74**, 3515 (1995);

L. Blanchet, Phys. Rev. **D54**, 1417 (1996); ibid. **D55**, 714 (1997);

P. Jaranowski and G. Schäfer, Phys. Rev. **D55**, 4712 (1997);

A. Gopakumar, B.R. Iyer and S. Iyer, Phys. Rev. **D55**, 6030 (1997); and Erratum: ibid. **D57**, 6562 (1998);

A. Gopakumar and B.R. Iyer, Phys. Rev. **D56**, 7708 (1997).

[24] T. Tanaka, H. Tagoshi and M. Sasaki, Prog. Theor. Phys. **96**, 1087 (1996).

[25] E. Poisson, Phys. Rev. **D52**, 5719 (1995).

[26] L. Blanchet, T. Damour, B.R. Iyer, C.M. Will and A.G. Wiseman, Phys. Rev. Lett. **74**, 3515 (1995); L. Blanchet, T. Damour and B.R. Iyer, Phys. Rev. **D51**, 5360 (1995); C.M. Will and A.G. Wiseman, Phys. Rev. **D54**, 4813 (1996); L. Blanchet, B.R. Iyer, C.M. Will and A.G. Wiseman, Class Quantum Gr. **13**, 575 (1996); L. Blanchet, Phys. Rev. **D54**, 1417 (1996).

[27] R. Arnowitt, S. Deser and C. W. Misner, Phys. Rev. **120**, 313 (1960).

[28] M. Davis, R. Ruffini, W.H. Press and R.H. Price, Phys. Rev. Lett. **27**, 1466 (1971); M. Davis, R. Ruffini and J. Tiomno, Phys. Rev. **D5**, 2932 (1972).

[29] W. Press, Astrophys J. Letters **170**, L105 (1971).

[30] R.H. Price and J. Pullin, Phys. Rev. Lett. **72**, 3297 (1994).

[31] J. Pullin, *The close limit of colliding black holes: an update*, Talk given at the Yukawa International Symposium at Kyoto, Japan, 1999 [gr-qc/9909021] and references therein.

[32] Z. Andrade and R. H. Price, Phys.Rev. **D 56**, 6336 (1997).

[33] S. Chandrasekhar and S. Detweiler, Proc. R. Soc. Lond. **A 344**, (1975) 441.

[34] E.W. Leaver, Proc. R. Soc. Lond. **A 402**, (1985) 285.

[35] F. Echeverria, Phys. Rev. **D40**, 3194 (1997).